

An Assessment of Dynamical Mass Constraints on Pre-Main Sequence Evolutionary Tracks

Lynne A. Hillenbrand and Russel J. White

*California Institute of Technology, Dept. of Astronomy/Astrophysics,
Mail Code 105-24, Pasadena, CA 91125, USA*

ABSTRACT

We have assembled a database of stars having both masses determined from measured orbital dynamics and sufficient spectral and photometric information for their placement on a theoretical HR diagram. Our sample consists of 115 low mass ($M < 2.0 M_{\odot}$) stars, 27 pre-main sequence and 88 main sequence. We use a variety of available pre-main sequence evolutionary calculations to test the consistency of predicted stellar masses with dynamically determined masses. Despite substantial improvements in model physics over the past decade, large systematic discrepancies still exist between empirical and theoretically derived masses. For main-sequence stars, all models considered predict masses consistent with dynamical values above $1.2 M_{\odot}$, some models predict consistent masses at solar or slightly lower masses, and no models predict consistent masses below $0.5 M_{\odot}$ but rather all models systematically under-predict such low masses by 5-20%. The failure at low masses stems from the poor match of most models to the empirical main-sequence below temperatures of 3800 K where molecules become the dominant source of opacity and convection is the dominant mode of energy transport. For the pre-main sequence sample we find similar trends. There is generally good agreement between predicted and dynamical masses above $1.2 M_{\odot}$ for all models. Below $1.2 M_{\odot}$ and down to $0.3 M_{\odot}$ (the lowest mass testable) most evolutionary models systematically under-predict the dynamically determined masses by 10-30% on average with the Lyon group models (e.g. Baraffe et al. 1998) predicting marginally consistent masses *in the mean* though with large scatter. Over all mass ranges, the usefulness of dynamical mass constraints for pre-main sequence stars is in many cases limited by the *random* errors caused by poorly determined luminosities and especially temperatures of young stars. Adopting a warmer-than-dwarf temperature scale would help reconcile the *systematic* pre-main sequence offset at the lowest masses, but the case for this is not compelling given the similar warm offset at older ages between most sets of tracks and the empirical main sequence. Over all age ranges, the systematic discrepancies between track-predicted and dynamically determined masses appear to be dominated by inaccuracies in the treatment of convection and in the adopted opacities.

Subject headings: (stars:) binaries (stars:) Hertzsprung-Russell diagram stars: pre-main-sequence

1. Introduction

Three of the most fundamental stellar parameters are mass, angular momentum, and composition, which together determine almost exclusively the entire evolutionary history of any given (single) star. Although stars spend the vast majority of their lives on the main sequence of hydrogen-burning, particularly interesting stellar objects are often those in the shorter-lived pre-main sequence or post-main sequence evolutionary phases. Our focus here is on the inference of stellar masses for pre-main sequence and young main sequence objects, for which observational data relevant to their location in the Hertzsprung-Russell (HR) diagram has become abundant in recent years. Masses and ages are often inferred from such HR diagrams via comparisons to an increasingly large suite of pre-main sequence evolutionary calculations. Instead of adopting a main sequence mass-luminosity relationship, one explicitly accounts for the evolution of the mass-luminosity relationship with age. The inferred stellar masses and ages are then used to construct initial mass functions and to surmise star formation histories of molecular clouds.

The pre-main sequence luminosity and effective temperature evolution of just-born stars was first calculated over a range of masses by Iben (1965) and by Ezer and Cameron (1967a,b) who assumed homologous contraction and solved the equations of stellar structure following the formalism of pioneers Henyey and Hayashi. Substantial improvements in the input physics and opacities was achieved during the following decades by several others, notably Vandenberg (1983) and D’Antona & Mazzitelli (1985). In the 1990’s several series of papers by different groups incorporated yet more complex and varied assumptions regarding the equation of state, opacities, convection physics, outer boundary condition of the stellar interior, and treatment of atmospheres. Electronically available data from these calculations including those from Swenson et al. 1994 (S93); D’Antona & Mazzitelli 1994 (DM94) and 1997 (DM97); Forestini 1994, Siess et al. 1997, and Siess et al. 2000 (S00); Baraffe et al. 1998 (B98) and Chabrier et al. 2000; Palla & Stahler 1993 and 1999 (PS99); and finally Yi et al. 2003 (Y²) were widely circulated. Other authors such as Burrows et al. 1997 and Baraffe et al. 2002 have focussed on sub-stellar mass objects.

Complications to simple luminosity and effective temperature evolution via radial contraction are the effects of rotation, composition, accretion, magnetic fields, and the presence of dust in the atmospheres of the lowest mass stars and brown dwarfs. These have been explored in limited capacity as well, as discussed by Mendes et al. (1999), D’Antona et al. (2000), Baraffe et al. (2002), and Siess et al. (1997a,b). In addition, the “zero point” or initial mass-radius relationship from which pre-main sequence evolution begins is poorly constrained (see Larson, 1972; Stahler 1983; Mercer-Smith, Cameron, & Epstein 1984; Palla & Stahler, 1993; Bernasconi 1996; Hartmann, Cassen, Kenyon 1997; Baraffe et al. 2002). In addition, comparison between data young cluster data and isochrones, including the predictions from lithium burning, show inconsistencies which lead us to infer that ages younger than ~ 10 Myr are particularly uncertain, and masses are also likely biased. Despite the large uncertainties and indeed the cautions offered by many of the above authors themselves regarding the utility of their models in explaining observations, the existing array of models has been used heavily over the past decade for comparison to the H-R diagrams assembled

for pre-main sequence stars in nearby star-forming regions. These tracks are the primary tool used to determine the ages and masses of young stars, and thus a cornerstone on which the conclusions of many star formation studies rest. Two examples are the interpretation of observational data in a meta-context such as the initial mass function or the star formation history of a particular region, or the evolution of circumstellar disks or stellar angular momentum through the pre-main sequence. Such conclusions rely entirely on the evolutionary models and systematically different results can arise from the use of different models.

Fundamental calibration of pre-main sequence evolutionary tracks is, however, not yet established. Several tests have been proposed. The predicted masses can be compared to those inferred from either binary orbits (e.g. Casey et al. 1998; Covino et al. 2000; Steffen et al. 2001) or velocity profiles of rotating circumstellar disks (e.g. Simon et al. 2000; Dutrey et al 2003). The predicted ages can be compared under the assumption of co-eval formation, to loci of pre-main sequence binaries (e.g. Hartigan, Strom, & Strom 1994; Prato, Greene, & Simon 2003), higher order multiples (White et al. 1999) and young “star-forming” clusters (e.g. Luhman et al. 2003; Hillenbrand, Meyer, & Carpenter 2004). Older open clusters offer even narrower sequences for comparison with model isochrones (e.g. Stauffer, Hartmann & Barrado y Navascues 1995). All of these tests, however, are limited by the accuracy with which individual stars can be placed on a theoretical H-R diagram. In addition to the poorly understood observational errors, uncertainties in the temperature and bolometric correction scales themselves remain significant, especially at sub-solar masses and young ages.

In this paper we explore the consistency of the masses predicted by various sets of pre-main sequence evolutionary tracks with those masses fundamentally determined from orbital dynamics. Our sample is larger than those considered in previous experiments (referenced above); in particular we include both pre-main sequence and main sequence stars. The lower mass limit in our sample is imposed by the available fundamental mass data ($0.1 M_{\odot}$ for main sequence stars but only $0.3 M_{\odot}$ for pre-main sequence stars) and the upper limit ($2.0 M_{\odot}$) is adopted to include only un-evolved main sequence objects.

In section 2 we discuss the models we test and the systematic differences between them. Section 3 presents the database of double-lined binaries or single/multiple stars harboring rotating gaseous disks with determined stellar masses, and our methodology for inferring masses from pre-main sequence evolutionary calculations. In section 4 we perform the detailed comparison of the model masses and the dynamically-determined fundamental masses. Section 5 contains our conclusions and recommendations.

2. Pre-Main Sequence Evolutionary Models

The various sets of tracks available and their most basic input assumptions regarding stellar interior structure and physics are reviewed in this section. In our analysis we make use of those sets

of models which have been made available electronically by the authors. We refer the interested reader to the references cited for more detail on individual sets of calculations. We do not attempt to assess the physical validity, triumphs, or shortcomings of the individual models; we present them purely for consideration in comparison to stellar masses fundamentally determined based on astrophysical data.

2.1. Victoria Group: S93

The heritage of the Swenson et al. models resides in the Victoria stellar evolutionary code of Vandenberg (1983; 1992). The notation “S93” refers to a private communication in 1993 of approximately the series F models described in Swenson et al. 1994, provided initially to K. Strom and subsequently to the present authors. The mass range covered is 0.15-5.00 M_{\odot} . These models employ the OPAL (Rogers & Iglesias 1992) and Cox & Tabor (1976) opacities, an “improved” Eggleton, Faulkner, & Flannery (1973) equation of state, Fowler et al. (1975) and Caughlan & Fowler (1988) reaction rates, use a mixing length parameter $\alpha = 1.957$, and assume abundances $Y = 0.282$ and $Z = 0.019$. Their starting point is defined as $\rho < 0.01 \text{ g/cm}^3$. Atmospheric treatment is presumed grey. A hint provided in Vandenberg & Clem (2003) suggests that more may be coming from this group on pre-main sequence evolution including realistic atmospheres, with the most recent description of main sequence and post-main sequence evolution appearing in Vandenberg et al. (2000).

2.2. D’Antona and Mazzitelli: DM94 and DM97

D’Antona & Mazzitelli (1994) provided tracks covering is 0.1-2.5 M_{\odot} using the first substantial improvement to input physics since the 1980’s pre-main sequence evolutionary papers which utilized 1970’s era physics. The models employ the Alexander et al. (1989) or Kurucz (1991) and Rogers & Iglesias (1992) opacities, Mihalas et al. (1988) and Magni & Mazzitelli (1979) equation of state, Caughlan & Fowler (1988) and Fowler et al. (1975) reaction rates, use either a mixing length parameter $\alpha = 1.2$ or the newly introduced Canuto & Mazzitelli (1991, 1992) “full spectrum of turbulence” (FST) convection prescription as a rival to the standard mixing length theory (MLT), and assume abundances $Y = 0.285$ and $Z = 0.018$. Atmospheric treatment is grey. Their starting point is the sequence of deuterium burning. These models were updated to cover 0.017-3.00 M_{\odot} in D’Antona & Mazzitelli 1997 (DM97) and again in 1998 (the later being a “web-only” correction at $< 0.2 M_{\odot}$ to the originally circulated 1997 models). As this article went to press we became aware of the Montalbán et al. (2004) calculations which explore both MLT and FST convection and now use the non-grey Hauschildt, Allard, & Baron (1999) or the Heiter et al (2002) a.k.a. Kurucz atmospheres. These models are not electronically available at present and are not used in our analysis.

2.3. Geneva group: C99

The Charbonnel et al. 1999 models cover 0.4-1.0 M_{\odot} and represent an extension to lower masses of the Geneva code. They employ the MHD (Hummer & Mihalas 1988; Mihalas et al. 1988; Dappen et al 1988) equation of state, the Alexander & Ferguson (1994) and Iglesias & Rogers (1996) opacities, Caughlan & Fowler (1988) reaction rates, a mixing length parameter $\alpha = 1.6$, and abundances $Y = 0.280$ and $Z = 0.020$. The atmospheric treatment down to $\tau = 2/3$ is grey. These models are not publicly available and are not utilized in the present study.

2.4. Palla and Stahler: PS99

The Palla & Stahler (1999) models over 0.1-6.0 M_{\odot} use the Rosseland mean opacity, the Eggleton, Faulkner, & Flannery (1973) and Pols et al (1995) equation of state, Fowler et al. (1975) and Harris et al. (1983) reaction rates, a mixing length parameter $\alpha = 1.5$, and assume abundances $Y = 0.28$ and $Z = 0.02$. The calculations explicitly include a “birthline” or initial mass-radius relationship (which, incidently, could be adopted and independently applied by any of the other calculations reviewed in this section). Atmospheric treatment is grey. These models do not extend beyond ages of 10^8 years.

2.5. Grenoble group: S00

The Grenoble group has published their calculations in Forestini 1994, Siess et al. 1997, and most recently in Siess et al. 2000 (S00). The calculations cover 0.1-7.0 M_{\odot} . They use the Alexander & Ferguson (1994) and Iglesias & Rogers (1996) opacities, a modified Pols et al. (1995) scheme for the equation of state, Caughlan & Fowler (1988) reaction rates, a mixing length parameter $\alpha = 1.6$, and abundances $Y = 0.288$ and $Z = 0.0189$. These models attempt to include a “realistic” atmosphere as the outer boundary condition using data from Plez (1992) and Kurucz (1991).

2.6. Lyon group: B98

The Lyon group published models in Baraffe et al. 1995, Chabrier & Baraffe 1997, and Baraffe et al. 1998 (B98). The calculations cover 0.035-1.2 M_{\odot} ; see Chabrier et al. 2000 and Baraffe et al. 2002 for an extension to 0.001 M_{\odot} . The Lyon group uses the Alexander & Ferguson 1994 and Iglesias & Rogers 1996 opacities, the Saumon, Chabrier, & van Horn 1995 equation of state, reaction rates described in Chabrier & Baraffe 1997, several different values for the mixing length parameter $\alpha = 1.0, 1.5, \text{ and } 1.9$, and abundances $Y = 0.275, 0.282$ and $Z = 0.02$. These models also employ the non-grey Hauschildt, Allard, & Baron (1999) atmospheres which include molecular opacity sources such as TiO and H₂O, as well as dust grains. It should be noted that the $\alpha = 1.9$

models are actually the same as the $\alpha = 1.0$ ones below $0.6 M_{\odot}$, and also that the $\alpha = 1.9$ models actually use $\alpha = 1.0$ in the atmospheres, at optical depths <100 . The B98 models do not extend to radii larger than those defined by the 10^6 year isochrone limiting their utility in studies of young low-mass star-forming regions where populations are frequently found above the limit of the B98 tracks.

2.7. Yale group: Y² and YREC

The Yale group has two current sets of models, one called “Y²” and the other “YREC” which includes rotation.

The Y² models cover $0.4\text{-}5.0 M_{\odot}$ and have been published in a series of papers: Yi, Kim, & Demarque 2003; Kim et al. 2002; Yi et al 2001. These models use Iglesias & Rogers 1996 and Alexander & Ferguson 1994 opacities, the Cox & Giuli 1968 and Rogers et al. 1996 equation of state with implementation of the Debye-Huckel correction (Guenther et al. 1992), reaction rates from Bahcall & Pinsonneault 1992, a mixing length parameter $\alpha = 1.7431$, and a range of abundances where we have chosen the $X = 0.71$, $Y = 0.27$, $Z = 0.02$ models for comparison. Atmospheres are presumed grey but for the purpose of calculating colors (not relevant to the present study) are matched in a semi-empirical way to the color-temperature relations adopted by Lejeune et al. (1998)¹. These models begin at the theoretically defined deuterium burning main sequence.

The YREC (Yale Rotating Evolution Code) models cover $0.1\text{-}2.25 M_{\odot}$ and have been published in Guenther et al 1992 and Sills, Pinsonneault, & Terndrup 2000. Currently these models also use Iglesias & Rogers 1996 and Alexander & Ferguson 1994 opacities, the Rogers et al. 1996 but also the Saumon, Chabrier & Van Horn 1995 equations of state as appropriate, reaction rates from Gruzinov & Bahcall 1998, a mixing length parameter $\alpha = 1.72$, and abundances corresponding to $Y=0.273$ and $Z= 0.0176$ at the age of the Sun. The atmospheric treatment is the same as Y². These models are not publicly available and are not utilized in the present study.

2.8. Comparison of Models and Systematic Effects

As illustrated by the above discussion of the gamut of pre-main sequence evolutionary models, there is substantial variation in the treatment of various aspects of the physics as well as in the adopted values of certain parameters. The most salient of these differences are in the opacity sources, treatment of convection, and treatment of interior/atmospheric boundary conditions. For comparison between the results of several of the above-mentioned codes at low masses, we show in Figure 1 the predicted contraction of different stellar masses, and in Figure 2 the resulting zero-age

¹We note specifically that the V-K vs $\log T_{eff}$ relationship given in Lejeune et al. does not place the M dwarfs in the present study on the main sequence, but rather substantially warmer and fainter than the main sequence.

main sequence as defined in Section 3.4. Systematic differences are apparent in the mass tracks, especially at young ages, and on the main sequence, particularly at low masses. The variations between tracks are predominantly in temperature and only secondarily in luminosity.

The predicted effective temperature for a given mass star is dictated largely by the treatment of convection in both the atmosphere and the interior. Because of the extreme complexity of a realistic prescription, convection is usually handled by adopting the mathematically simple mixing-length theory (Böhm-Vitense 1958), although more sophisticated prescriptions have been proposed (e.g. Canuto & Mazzitelli 1992). Typically, larger mixing lengths (more efficient convection) predict hotter evolutionary tracks and yield lower masses for a given position in the HR diagram. The choice of the mixing length is a large uncertainty in current models. A common value is one which predicts $1 M_{\odot}$ model agreement with the solar model, but this approach may artificially compensate for other inadequacies in the calculations. For example, several other major aspects of convection can affect the track temperatures such as how the interior is matched to atmosphere, the thickness of the convective region, and the extent of convective overshooting (see e.g. D’Antona & Mazzitelli 1994; Montalbán et al. 2004). Consequently, the treatment of convection is one of the primary uncertainties in current evolutionary models. A related effect is the opacity (including the influence of metallicity) through which the convective energy transport must occur. Higher opacities generally mean lower predicted effective temperatures for a given mass star.

Another point of comparison between sets of models is the match between the various $1 M_{\odot}$ tracks and the location of the Sun. The Sun is evolved from its zero-age main sequence location being hotter, larger, and more luminous. In some cases certain parameters in the above sets of models have been adjusted by the model authors such that their $1 M_{\odot}$ model reproduces the temperature and luminosity of the present day Sun. This requires that the model tracks extend beyond the zero-age main sequence. Nevertheless, we illustrate in Figures 1 and 2 the location of the Sun compared to $1 M_{\odot}$ pre-main sequence tracks and zero-age main sequences (effectively the 10^8 year isochrone at this mass; see §3.4) from various models. This comparison notwithstanding, we demonstrate in our results that there is little correspondence between models being able to match the observed main sequence parameters and the observed pre-main sequence parameters.

Finally, it should be stressed that there is generally poor agreement between the various models and the empirical main sequence at low masses (Figure 2). Of note is that the Y^2 models which at low masses do seem to reach as cool as the empirical data, do not display the same downturn at low temperatures as other models. A downturn, such as that displayed by the S93 models in the same cool regime, and by the other models at much warmer temperatures, is expected based on the dissociation of H_2 (Copeland et al 1970).

3. Astrophysical Data

3.1. Sample and Selection Criteria

In order to test the predictions of the various pre-main sequence evolutionary tracks just discussed, we have compiled from the literature a list of stars with dynamically determined masses and with luminosity and temperature estimates for placing them on the HR diagram. The sample is restricted to stars less massive than $2.0 M_{\odot}$. Of the 148 stars in this sample (Table 1), 88 are main-sequence and 27 are pre-main sequence stars; the remaining 33 stars are determined to be post-main sequence as described below. The Sun is included as a main sequence star with stellar parameters adopted from Gray (1992).

For the main sequence sample we require masses measured to better than 10%. We strive to exclude W UMa type contact binaries (e.g. V781 Tau; Liu & Yang 2000) in which tidal effects or mass transfer could be important. Further, to avoid including stars evolved too far beyond the zero-age main-sequence (ZAMS), we have retained for analysis only those binary components in Table 1 with $\log g > 4.20 \text{ cm sec}^{-2}$, and thus stars less evolved than $\sim 600 \text{ Myr}$ from the ZAMS near our upper mass range and less evolved than 1-3 Gyr from the ZAMS near the solar mass range (according to the Girardi et al. 2000 post-ZAMS models). We begin with the catalog of Anderson (1991) and the additional lists compiled by Ribas (2000), Delfosse et al. (2000), and Lastennet & Valls-Gabaud (2002), but also include systems more recently identified in Munari et al. (2001), Zwitter et al. (2003), and Marrese et al (2003). Of the compiled systems surviving our selection criteria, most are detached double-lined eclipsing binaries. The remaining main-sequence stars are spatially resolved double-lined spectroscopic binaries which have independent temperature estimates for each component from spectroscopic or color measurements that enable their placement on the HR diagram. We note that the main-sequence sample of stars suitable for our purposes has, historically, been biased towards solar or greater masses. In recent years, however, the sample of stars at masses $< 0.5 M_{\odot}$ with both dynamical masses and independent temperature and luminosity estimates for the two components has grown considerably (e.g. Delfosse et al 2000).

The pre-main sequence sample is not subjected to the same dynamical mass uncertainty restriction that is applied to the main sequence sample ($\sigma < 10\%$) due to the small numbers of stars having measured masses. These 27 pre-main sequence stars include 8 components of double-lined eclipsing binary systems (TY Cr Ab, EK Cep B, RS Cha A & B, RXJ0529.4+0041 A & B, AK Sco A & B; see references in Table 1) which have the most accurately determined masses among the pre-main sequence sample ($\sigma \leq 5\%$), but are all approximately solar or larger mass stars. One pre-main sequence system has component masses determined from spatially resolved measurements of a double-lined spectroscopic binary (NTTS 045251+30016 A & B; Steffan et al. 2001). Nine pre-main sequence stars have masses determined from disk kinematics (Simon et al. 2000; Dutrey et al. 2003). In the case of the UZ Tau E binary, the component masses are determined from the spectroscopic orbit inferred by Prato et al. (2002). The remaining pre-main sequence systems (FO Tau, FS Tau, DF Tau, GG Tau) are all binaries which have only total dynamical mass estimates;

in these cases we thus compare these total dynamical masses to the summed masses inferred from placement of the individual components on the HR diagram. Although other pre-main sequence binary systems have orbital mass estimates, we include only those which have spatially resolved temperature or spectral type measurements. We do not include systems with only mass ratios available.

3.2. Stellar Parameters I: Mass, Radius and Surface Gravity

The sample is listed in Table 1 in order of the most to the least massive star and with pre-main sequence stars distinguished from main sequence stars. The mass and radius range occupied by the un-evolved members of our sample ($\log g > 4.20 \text{ cm sec}^{-2}$) is shown in Figure 3. For stars which are members of eclipsing systems, radii are determined directly from observations; for the remainder this quantity has been estimated for plotting purposes from temperature and luminosity following Stefan’s Law ($L = 4\pi R^2 \sigma T_{eff}^4$). In the remainder of this section we describe how the masses, radii, and gravities listed in Table 1 were derived by the original authors.

For the double-lined eclipsing binaries, the ratio of velocity amplitudes is inversely proportional to the ratio of masses while the sum of velocity amplitudes is related via the period to the sum of the masses. Given two equations and two unknowns, the individual component masses can thus be determined directly from the observables v_1 , v_2 , and the orbital period. Photometric measurements of the eclipse provide the ratio of radius to semi-major axis while the assumption of ≈ 90 degree system inclination means that radial velocity measurements yield the semi-major axis uniquely and hence one can solve for the radius directly from the observations (e.g. Covino et al. 2000). Double-lined eclipsing binary systems are the only binary systems with radius estimates determined directly from observables. The radii combined with the masses yield surface gravities ($g = GM/R^2$). Only those radii and surface gravities determined from fundamental observables are listed in Table 1.

For the spatially resolved double-lined systems, one does not have the benefit of knowing the system inclination. Instead, one can constrain the inclination via a combined astrometric and radial velocity orbital solution, allowing the individual masses to be recovered (e.g. Steffen et al. 2001). For spatially resolved binaries with an astrometric orbital solution but no radial velocity orbital solution, a total system mass can be determined if a distance is assumed (e.g. Schaefer et al. 2003). Finally, for stars surrounded by spatially resolvable circumstellar gas disks, interferometric measurements which map the velocity profile can be used to dynamically determine the central mass under the assumption of keplerian motion (e.g. Simon et al. 2000). In some cases, the central mass may a binary star.

3.3. Stellar Parameters II: Temperature and Luminosity

Comparison of the dynamically determined masses discussed above with those inferred from theoretical calculations requires temperature and luminosity information for every star. In determining these values, we apply the same methods to both the main-sequence and the pre-main sequence samples. For the eclipsing binary systems, the ratio of the stellar temperatures are typically determined very precisely from light curve analysis (see individual references cited in Table 1). These values are then combined with a mean system temperature estimated from photometrically calibrated atmospheric models (see e.g. Ribas et al. 2000), to determine individual effective temperatures². Although the temperatures listed in Table 1 are all taken directly from the references and thus in many cases are determined in a non-uniform fashion, we have in all cases adopted the values which use the most recent and accurate photometric calibrations. Since the stellar radius is also a quantity inferred from light curve analysis, luminosities are then determined directly from Stefan’s law and are, for most part, distance independent. In some cases we transformed quoted M_{bol} values to $\log L$ values. We assume $M_{bol(\odot)} = 4.75$ mag in all calculations (Allen & Cox 2000; see also footnote #7 in VandenBerg et al. 2000).

For the remaining (non- double-lined eclipsing) main sequence stars, we determine temperatures in one of 3 ways. Preferably, we adopt temperatures and uncertainties from the listed references when they are determined from a line ratio analysis (e.g. Gray 1994). Alternatively, we estimate the temperatures from the spectral types or, if no spectroscopic information is available, we determine the temperature from the observed photometric colors. We use the temperature / spectral type / color relations listed in the Appendix and assume an uncertainty in $\log T$ of 0.015 dex, which corresponds to roughly 1 spectral subclass, despite that the formal errors in $\log T$ based on color errors would be substantially smaller. Temperatures determined from either spectral types or colors are listed in italics in Table 1 as they are not fundamental temperature measurements. Luminosities are recalculated here based on optical or infrared photometry, bolometric corrections from the Appendix, and distance estimates. All of the main-sequence stars have parallax information, and hence distances. Although the luminosities are recalculated to ensure no systematic errors from different assumptions, we generally adopt the published luminosity uncertainties. For the stars with only spatially resolved photometry, we adopt a uniform uncertainty in $\log L$ of 0.05 dex.

For the remaining (non- double-lined eclipsing) pre-main sequence stars, temperatures are determined from spectral synthesis in the case of BP Tau (Johns-Krull et al. 1999), or from spectral types and the temperature relation listed in the Appendix, assuming an uncertainty of 0.015 dex. Photometric colors alone are insufficient for estimating the temperatures of pre-main sequence stars because of possible extinction and continuum excesses from either an accretion shock or the inner

²Several eclipsing systems are known to be chromospherically active binary stars (e.g. Strassmeier et al. 1993) in which star spots are an unaccounted-for bias in the temperature estimates. These systems are noted as such (“CABS”) in Table 1.

circumstellar disk. The luminosities are calculated from I_c -band measurements, which are the least likely to be contaminated by possible continuum excesses, and are at an optimal wavelength from which to apply a bolometric correction for early A through mid-M spectral types. All pre-main sequence stars for which we have calculated luminosities are in Taurus; we assume a distance of 140 pc (Kenyon et al. 1994). Also for this sub-sample of young T Tauri stars, we assume a uniform uncertainty of 0.10 dex in $\log L$ which incorporates typical 1 spectral sub-class errors propagated to errors in intrinsic colors and in bolometric corrections used to calculate reddening-free luminosities.

3.4. Masses Estimated from Tracks

We derive track-predicted masses for our sample by interpolating between tabulated luminosity and effective temperature values as a function of stellar mass and age for each set of tracks we test. In practice, the methods adopted to determine masses for the main sequence and pre-main sequence stars differ slightly. For the pre-main sequence stars, isochrones are generated at log ages intermediate to those tabulated by the model authors. The mass is determined via interpolation along the isochrone that intersects with the stellar luminosity and temperature. For stars with luminosities that put them above the youngest isochrone, the mass is assigned using this youngest isochrone and the temperature. This occurs only for the B98 tracks and only for a few late-K and M type T Tauri stars. Uncertainties in the track-predicted masses are determined from the range of masses predicted by varying the luminosity and temperature estimates by their uncertainties as listed in Table 1.

For stars already on the main sequence where isochrones converge in the luminosity / effective temperature plane, we have created a theoretical young main sequence for each set of tracks by adopting the 10^8 year isochrone at masses of $0.7 M_\odot$ and above (such that stars have already arrived at their ZAMS position but have not yet begun any substantial evolution away from it) and the 10^9 year isochrone below this mass. Only objects less massive than $0.09 M_\odot$ have not reached the ZAMS by 10^9 years according to the models; the least massive main sequence star in our sample is $0.10 M_\odot$. We refer to Figure 2 for comparison of the luminosity / effective temperature relationship adopted as the main sequence for the various sets of tracks. These constructed main-sequences represent a unique mass-temperature and mass-luminosity relation for each model. We use these relations to determine the main-sequence masses by averaging, for each star, the mass determined from interpolation of the stellar temperature and that from interpolation of the stellar luminosity. Uncertainties are estimated from the uncertainties in the stellar properties (luminosity and temperature) and the difference between the luminosity-predicted and temperature-predicted masses. This procedure could not be followed for the PS99 tracks since no 10^9 year isochrone exists and the 10^8 year isochrone exists only in the mass range 0.1 - $0.8 M_\odot$; no main-sequence masses are determined from these models.

The validity of our adopted main-sequence isochrone merits some discussion. Since there is continuous luminosity and temperature evolution even when stars are on the main sequence, our

derived masses are appropriate, in a strict sense, only for the specific age assumed in creating the mass-luminosity or mass-temperature relationships. For example, at masses above $0.7 M_{\odot}$ where we have adopted the relationships for 10^8 years, a $1.0 M_{\odot}$ star will have its mass overestimated by 2% if it is really 10^9 years old while a $2.0 M_{\odot}$ star will have its mass overestimated by 10%. One might think about assuming for all stars in our main sequence sample the mean age in the solar neighborhood of ~ 3 Gyr. This approach would be incorrect, however, since we have selected stars via their surface gravity to be on the hydrogen-burning main sequence, which corresponds to different mean ages at different masses. If a star is really 3×10^9 years old it will not be in our main sequence sample at $2.0 M_{\odot}$, but at $1.0 M_{\odot}$ will have its mass overestimated by 6%. Without precise knowledge of the ages of the stars in our sample we can only bear these biases in mind; we can not correct for them. Because the hydrogen-burning main sequence is widest for the most massive ($> 10 M_{\odot}$) stars and decreases in width towards lower masses, this effect should not limit the conclusions drawn from our primarily low mass sample.

4. Comparison of Track Predicted Masses to Dynamical Masses

Figure 4 shows comparisons between the dynamically determined masses and the masses inferred from all eight sets of evolutionary tracks; both the direct correlation of mass and the difference between the two masses as a percentage of the dynamical mass are provided. Figure 5 shows the mean percentage differences between track-predicted and dynamical masses as a function of dynamically determined mass (essentially a binned version of the upper plots in Figure 4). The standard deviations of the means are plotted as error bars for statistical assessment. In both of these Figures the main-sequence and the pre-main sequence samples are distinguished. The binary systems which have only total system dynamical masses (FO Tau A/B, FS Tau A/B, DF Tau A/B, GG Tau Aa/b) have been plotted assuming that the average mass per star is $1/2$ the total dynamical mass and that the average offset per star is $1/2$ the total system difference. This assumption is justified given the similar spectral types of the components of these binaries (Table 1). Figures 4 and 5 illustrate the differences between the predictions of the various pre-main sequence evolutionary calculations and are now used to assess the robustness of the predicted stellar masses.

4.1. Main Sequence Stars

We first consider the comparison of the main sequence sample. For the 5 tracks that extend to the largest masses considered here, $1.2 - 2.0 M_{\odot}$ (S93, DM94, DM97, S00, Y²), there is excellent agreement between the theoretical and dynamically determined masses in all cases. Closer to $1.0 M_{\odot}$, the S93, DM94, DM97 and Y² models again predict main sequence masses that are consistent with dynamically determined values. However, both B98 models and the S00 models predict masses that are 5% (at $1-2 \sigma$) larger than the dynamical masses. This could be an evolutionary effect since the average age of the solar mass main-sequence stars in our sample is likely more than 10^8 years.

Note, however, that the Sun (indicated by the solar symbol) resides just beyond the one-sigma error in the mean difference, likely indicating that the Sun is slightly older than the mean $1 M_{\odot}$ star in our sample; as discussed in §3.4, the 10^8 yr isochrone will overestimate the mass of the Sun by 6%, roughly the magnitude of the observed offset. At sub-solar masses, all tracks except for S93 and Y^2 predict masses that are less than the dynamically determined values by 15-30% at several sigma significance. The Y^2 models show the flattest overall trend (see Figure 5) with agreement between predicted and dynamically determined masses to within 1-3% over all masses down to $0.6 M_{\odot}$; the agreement slips to 7% for the lowest considered mass of $0.4 M_{\odot}$. The S93 models, in contrast to other models at low masses, are consistent with dynamical masses down to $0.3 M_{\odot}$ but systematically *over-predict* (as opposed to under-predict) the lower masses. Near $0.1 M_{\odot}$ (the 2 lowest mass bins), all models that extend this low appear to reverse their offset trends and again predict masses that are consistent with the dynamically inferred values.

The systematic discrepancy of predicted and dynamical masses for $0.2 - 0.5 M_{\odot}$ main-sequence stars likely stems from the poor match of model 10^9 year isochrones (our adopted main-sequence over this mass range) with the empirical main-sequence, as shown in Figure 2. We note that this empirical main sequence is consistent with the location of low mass main-sequence members of our sample (Figure 3), confirming that these stars are not peculiar because of, for example, chromospheric activity. The DM97, B98, and S00 models, which all under-predict low-mass stellar masses, are either too hot by ~ 200 degrees or under-luminous by a factor of three. We note though that masses determined via interpolation of stellar luminosity are more consistent with dynamically determined values than the masses determined via interpolation of stellar temperature (the adopted values for comparison to dynamical masses are the average of the luminosity-predicted and the temperature-predicted masses; see §3.4). This suggests that the main source of discrepancy in the models is in temperature and not the luminosity.

A major cause of systematic disagreement between low-mass dynamical masses and track-predicted masses is disparity between observation and theory in the “break” in the mass-luminosity relationship (seen in the figures as a break in the temperature-luminosity relationship). In most models this break occurs at a hotter temperature ($\log T \sim 3.7$ dex; M0.5 spectral type) than the location of the empirical break ($\log T \sim 3.5$ dex; M3.5 spectral type). Even the Y^2 models, which predict the most consistent masses, are clearly diverging from the empirical main-sequence over this mass range; these models exhibit no break in their mass-luminosity (temperature-luminosity) relationship. Only the S93 models offer reasonable agreement with the empirical main-sequence at low masses. Interestingly, the standard deviation of the mean offset is much larger at low masses for the S93 models than for other models; this is because the data scatter uniformly around this main sequence whereas for other models the offset between the data and the predicted main sequence is large, and the standard deviation in the mean offset is substantially smaller since *all* the data are offset in the same direction and by roughly the same amount. Similar conclusions regarding the accuracy of the predicted main sequence can be derived by comparing open cluster loci to these models (e.g. Stauffer et al. 1995; Hillenbrand et al. 2004). At high masses, the divergence seen in

Figure 2 between the models and the empirical main sequence is expected since most main sequence stars (i.e. those used to derive the absolute and bolometric magnitudes of typical main sequence stars) are slightly more evolved than the theoretical ZAMS.

4.2. Pre-Main Sequence Stars

We now consider the pre-main sequence sample. Relative to our main sequence sample these stars have poorly constrained temperatures and luminosities, leading to larger errors in HR diagram placement and hence larger errors in predicted masses. In addition, the errors in the dynamical masses for this sample are often substantially larger than the 10% limit we imposed on the main sequence sample. Finally, the statistics for the pre-main sequence are comparatively worse given the small number of pre-main sequence stars with dynamically determined masses. With these caveats in mind, we interpret the comparisons shown in Figures 4 and 5 with the aid of Figure 6 which shows the results for individual stars, similar to the top panels of Figure 4, but with an expanded scale and now with individual error bars.

Above $1.2 M_{\odot}$, all models considered (all except both B98 calculations which do not extend above this mass) predict pre-main sequence masses that are consistent with dynamically determined values to better than 1σ in the mean (Figure 5), with the DM94 and DM97 tracks tending to under-predict the individual masses by 0-10%. Around $1 M_{\odot}$ (0.5 - $1.2 M_{\odot}$), the B98 $\alpha=1.0$ models predict masses most consistent with dynamical values; the B98 $\alpha=1.9$ and most other models predict masses that are too low by $\sim 25\%$ at $1-2\sigma$ on average compared to the dynamically determined values. This general trend of underpredicted masses continues (including for the B98 $\alpha=1.0$ models) towards the lowest pre-main sequence masses considered, $0.3 M_{\odot}$ though with slightly less significance ($\sim 1\sigma$). Note that the valley of maximum disagreement between track-predicted and dynamical masses is driven for all models by two stars: UZ Tau Aa and NTTS 045251 B.

Our assessment of these mass comparisons is limited by the accuracy with which our sample stars can be placed on an H-R diagram, particularly the youngest stars. As young solar- and lower mass stars are primarily on Hayashi (roughly constant temperature) evolutionary tracks, an accurate temperature is especially important for determining a theoretical mass. In our analysis we have adopted a dwarf temperature scale for both the main sequence stars and the pre-main sequence stars. Pre-main sequence stars are intermediate gravity objects between dwarfs and giants and it has been argued (e.g. Martín et al. 1994; Luhman et al. 1997; White et al. 1999) that the appropriate spectral type - temperature relation of, in particular T Tauri stars, should be intermediate between that of dwarfs and giants. G and K giants are cooler than G and K dwarfs, while M giants are warmer than M dwarfs (see Appendix for dwarf temperatures and Dyck et al. 1996, Di Benedetto & Rabbia 1987, and Bell & Gustaffson 1989 for giant temperatures derived from either angular diameters or the infrared flux method) with the crossover point at about M0. As examples, in comparison to dwarfs, giants of spectral type M6 are ~ 620 K warmer, M4 are ~ 500 K warmer, M2 are ~ 310 K warmer, K5 are ~ 475 K cooler, and K1 are ~ 595 K cooler. Detailed analysis of high

dispersion spectra shows that pre-main sequence surface gravities are closer to dwarfs than giants. For example, Johns-Krull et al. (1999) measure $\log g = 3.67 \pm 0.5$ for BP Tau and Johns-Krull & Valenti (2001) quote $\log g = 3.54$ for Hubble 4. These values can be compared to $\log g = 4.6$ for a 4800K dwarf and $\log g = 2.4$ for a 4800 K giant (dwarf surface gravities staying roughly constant with decreasing temperature in the stellar range and giant gravities decreasing by one order of magnitude by 3900 K and two orders of magnitude by late M spectral types).

In our analysis, we have assumed a strict dwarf-like temperature relation since an appropriate temperature scale tied to the infrared flux method or measured stellar angular diameters has not yet been established for 1-10 Myr low mass stars. The systematic shift induced by adopting a temperature scale intermediate to that of dwarfs and giants would make our track-inferred masses for the pre-main sequence stars *smaller* in the GK spectral type range (the wrong direction for improving correspondance to dynamical masses) and *larger* by $\sim 10\%$ for the M types. Luhman et al. (2003) suggest a specific intermediate temperature scale for stars cooler than spectral type M_0^3 . Using this warmer temperature scale for our pre-main sequence sample (filled squares in Figure 6) systematically increases the predicted masses of the lowest mass stars. However there is no statistically significant evidence from dynamical mass constraints that a warmer-than-dwarf temperature scale is needed since the resulting change in the predicted masses using a warmer scale is well within the uncertainties in the mass comparison plots (only 2 systems have masses shifted by $\geq 1\sigma$ via a change in the temperature scale).

Systematic shifts in the predicted masses, as would occur by shifting the temperature scale, will still leave many pre-main sequence stars with track-predicted masses widely discrepant from dynamical values. This is illustrated by the large scatter in track predicted masses over a small range of dynamically determined masses (Figure 6). A couple of case studies make this point clear. Compare MWC 480, an A2 star with dynamical mass of $1.65 \pm 0.07 M_\odot$, to the cooler but (surprisingly) more massive A8 stars RS Cha A & B, with dynamical masses of $1.858 \pm 0.016 M_\odot$ and $1.821 \pm 0.018 M_\odot$. No evolutionary model will predict that a hotter object is less massive than a cooler object this close to the main-sequence. Assuming that the uncertainties in the dynamical masses have been properly assigned, this suggests that the assigned temperatures are in error. In this case, the error is most likely in the spectral type assigned to MWC 480 since RS Cha is an eclipsing system with more precisely determined temperatures. Similar discrepancies occur at lower masses. Consider NTTS 04251+3016 A and LkCa 15, two K5 T Tauri stars with identical luminosities. Although these stars are located at the same position in the H-R diagram, they have dynamically determined masses that differ by $0.48 M_\odot$, a 2.5σ difference. This again strongly suggests errors in the assigned spectral types. These discrepancies are problems that will remain, independent of the temperature scale and independent of any evolutionary model. Assuming that the uncertainties in dynamical masses are being properly assessed, we conclude that usefulness

³The values of the Luhman intermediate temperature scale were chosen to produce co-eval ages for the T Tauri quadruple GG Tauri and for members of the IC 348 cluster using the B98 ($\alpha = 1.9$) evolutionary models.

of dynamical mass constraints on pre-main sequence evolutionary models is currently limited by poorly determined luminosities and especially temperatures of pre-main sequence stars.

4.3. Ensemble Comparisons

Finally, in assessing the main sequence and the pre-main sequence results en ensemble, we find it somewhat distressing that for most models the agreement for main sequence masses is far better than for pre-main sequence masses. Assuming the stellar parameters on average are well understood (the above exceptions notwithstanding), apparently it is possible for stars of given mass to wind up in the right place near the main sequence end of a calculation without having started them in the right place at the tops of their convective evolutionary tracks.

The B98 ($\alpha=1.0$) models appear to have the best consistency between the pre-main sequence and main sequence mass offsets as a function of mass (Figure 5), though we remind the reader that we found the B98 $\alpha=1.0$ models a better fit to the pre-main sequence and the B98 $\alpha=1.9$ models a better fit to the main sequence. If this trend is proven true, it may indicate a difference in the efficiency of convection between pre-main sequence and main sequence stars of similar mass. As noted above, for all models there is indeed *consistency* above $1.2 M_{\odot}$ in both the pre-main sequence and the main sequence phases with dynamical masses; however, the pre-main sequence masses are systematically offset by 0-30% ($< 1\sigma$). Below $1 M_{\odot}$ the consistency between the pre-main sequence and main sequence masses is broken, with the offset masses in the two regimes different in most models by $> 1\sigma$. Notably it is in this sub-solar regime where convection is most important, and for an increasingly longer time period towards lower masses, during pre-main sequence evolution.

5. Conclusions and Recommendations

We have attempted to assess the agreement between dynamically determined stellar masses and those inferred from modern theoretical calculations of pre- and early-main sequence evolution. We have found only marginal consistency with most existing models, as summarized in Figure 5.

For main-sequence stars, above $1.2 M_{\odot}$ the models considered are all consistent with dynamically determined values. At lower masses, however, there is divergence between the predicted and dynamical masses which sets in at different masses for different tracks. The Y^2 models offer the best overall agreement with dynamical masses, though these calculations extend only as low in mass as $0.4 M_{\odot}$. The S93 models are a close second to the Y^2 models but begin to diverge from 1σ consistency below $0.3 M_{\odot}$. All other models (DM97, B98, S00, and PS99) fail to predict masses that are consistent with dynamically determined values (by 5-20%) over the mass range $0.1 - 0.5 M_{\odot}$. We find that for all tracks, the dominant discrepancies between track-predicted and dynamically determined masses for main-sequence stars lie in the mass range 0.2 to $0.5 M_{\odot}$. This failure likely stems from the poor match to the empirically defined main-sequence. The DM97, B98, PS99, and

S00 models all predict a break in the mass-luminosity relationship near $\log T \sim 3.7$ dex (spectral type M0.5), which is hotter than the well established empirical break in the mass-luminosity relationship near $\log T \sim 3.5$ dex (spectral type M3.5). The S93 and Y² models most closely resemble the empirical main sequence.

For the pre-main sequence sample, we find generally good agreement between predicted and dynamical masses above $1.2 M_{\odot}$ for all models, as was true for the main sequence sample. This is not an entirely trivial statement since both partially convective and fully radiative stars are included between these two samples. However, referring to Figure 1, differences between the various models for $1-2 M_{\odot}$ stars are manifest only high on the fully convective part of the tracks where no empirical data exists; thus even younger $1-2 M_{\odot}$ dynamical masses are needed before distinction between the pre-main sequence tracks can be made in this mass regime. Between 1.2 and $0.5 M_{\odot}$, the B98 ($\alpha=1.0$) models predict *reasonably* though not fully consistent mass values on average, while all other models systematically underestimate sub-solar masses by 10-30% on average. At the lowest masses considered, $\lesssim 0.5 M_{\odot}$, all models underestimate pre-main sequence stellar masses. There are at present no dynamical mass constraints available at masses less than $0.3 M_{\odot}$ for pre-main sequence stars. Adopting a warmer-than-dwarf temperature scale for T Tauri stars could partly reconcile these mass under-estimates, though the scale proposed by Luhman et al. (2003) is not warm enough to rectify the mass underestimates except for the marginal (that is, not statistically significant) improvements made to the B98 model agreement (the models to which this temperature scale was in fact tuned). With the above caveats in mind, we find that the B98 $\alpha=1.0$ models used with a slightly warmer-than-dwarf temperature scale predict pre-main sequence masses that agree the most consistently with dynamically determined values. Of note is that the B98 models do not extend above radii of $1-2 R_{\odot}$ (specifically the 10^6 year isochrone) whereas many young pre-main sequence stars have larger radii, $2-3 R_{\odot}$, thus limiting the utility of the B98 models in star-forming regions. The dynamical mass consistency of the B98 models is only marginally better than the DM97, PS99, and S00 models, which systematically underestimate sub-solar masses by $1-2\sigma$.

The relatively flat nature of the offsets between the dynamical and the predicted stellar masses for some calculations suggests that they could be used with moderate confidence if correction factors are included. For example, a 20% revision upward of the masses predicted by the DM97 tracks for masses between $0.12-0.4 M_{\odot}$ would result in near-perfect agreement at main sequence evolutionary stages, with the same 20% correction applicable to $0.3-1.0 M_{\odot}$ young pre-main sequence stars; again we note that the pre-main sequence behavior below $0.3 M_{\odot}$ is untested for these or any set of tracks. A similar 20% correction could be applied to the S00 pre-main sequence tracks, though the main sequence offsets appear to vary with mass.

Several observational recommendations can also be made. Our pre-main sequence comparisons stress the need for more observational work on masses determined from orbital dynamics in the pre-main sequence phase where the statistics of our assembled sample are factors of 5-10 worse than on the main sequence at comparable masses. This is especially problematic at the lowest masses where at present there are no pre-main sequence dynamical mass constraints at masses $<0.3 M_{\odot}$. Finally,

we emphasize that the usefulness of dynamical mass constraints on pre-main sequence evolutionary models are currently limited by poorly determined luminosities and especially temperatures of young stars. Additional dynamical mass determinations will not likely improve the constraints on evolutionary models unless the stellar parameters can be more accurately determined than for the current sample. In the absence of additional eclipsing systems, high dispersion stellar spectroscopy and synthetically modeled spectra offer the best promise for precisely determining fundamental properties.

The trends that have emerged from our study may be interpretable as messages regarding modifications to the model assumptions on input physics and parameter choices. It is suggested that in order to achieve agreement between dynamical and track-predicted masses for both low-mass young pre-main sequence stars and main sequence stars, a systematic shift coolward of the models via improved convection and opacity treatments are needed. Further adjustments may also be necessary. Baraffe et al. have repeatedly stressed the important effects of atmospheres at low masses, arguing that the grey (Eddington) approximation used by most other authors overestimates both the temperature and the luminosity for a given mass. This in part could explain some of the discrepancies between the predicted and empirical main-sequences (Figure 2). It is worth noting that the deviations occur near early M spectral types, where molecular absorption begins to dominate the opacity. However, even the non-grey atmospheres of the B98 models fail to reproduce the empirical main-sequence. For the pre-main sequence stars, although the physics involved in opacities, equations of state, and atmospheric treatment is already challenging, even more sophisticated effects such as accretion, rotation, and magnetic fields may be required in order to achieve rigorous agreement between observations and models, as illustrated by e.g. D’Antona et al. 2000 and Baraffe et al. 2002.

We acknowledge useful comments by the referee.

A. Adopted Dwarf Temperatures and Bolometric Corrections

As discussed in the text (§3.3 and 4.2), we have adopted a dwarf temperature scale based on the stellar temperatures of Chlebowski & Garmany 1991 (O3-O9); Humphreys & McElroy 1984 (B0-B3); Cohen & Kuhi 1979 (B5-K6); Bessell 1991 (K7-M1); Wilking, Greene, Meyer 1999 (M2-M7.5); and Reid / Burgasser (M8-L-T). Our bolometric corrections are those of: Massey et al. 1989 (O3-B1); Code et al. 1976 (B2-G0); Bessell 1991 and Bessell & Brett 1988 (G0-M5); and Tinney, Mould, & Reid 1993 (M6-M9, converted from quoted values of BC_K). The V-band bolometric corrections turn over at spectral types later than late-G, and grow rapidly as flux shifts from the V-band into redder band passes. I-band is generally the best wavelength at which to apply a bolometric correction for stars in the early-K through mid-M spectral type range, both because the value of the bolometric correction is small and because it is roughly constant with spectral type. For very late M-types the J-band may be a better choice.

REFERENCES

- Alencar, S.H.P., Melo, C.H.F., Dullemond, C.P., Andersen, J., Batalha, C., Vaz, L.P.R., & Mathieu, R.D. 2003, AA, 409, 1037
- Alexander, D.R., Augason, G.C. & Johnson, H.R. 1989, ApJ, 345, 1014
- Alexander, D.R. & Ferguson, J.W. 1994, ApJ, 437, 879
- Allard, F., Hauschildt, P.H., Alexander, D.R., Starrfield, S. 1997, ARAA, 35, 137
- Allen, C.W. & Cox, A.N. Astrophysical Quantities 2000 (New York: Springer-Verlag)
- Andersen, J. 1991, A&A Rev., 3, 91
- Andersen, J., Lindgren, H., Hazen, M. L. & Mayor, M. 1989, A&A, 219, 142
- Bahcall, J.N. & Pinsonneault, M.H. 1992, Rev. Mod. Phys. 60, 297
- Baraffe, I., Chabrier, G., Allard, F., & Hauschildt, P. H. 1995, ApJ, 446, 35 (B95)
- Baraffe, I., Chabrier, G., Allard, F., & Hauschildt, P. H. 1998, AA, 337, 403 (B98)
- Baraffe, I., Chabrier, G., Allard, F., & Hauschildt, P.H. 2002
- Basri, G. & Batalha, C. 1990, ApJ, 363, 654, 669
- Bell, R.A. & Gustaffson, B. 1989 MNRAS 236, 653
- Bernasconi, P.A. 1996, A&AS, 120, 57
- Bessell, M.S. 1991, ApJ 101, 662
- Bessell, M.S. & Brett, J.M. 1988, PASP 100, 1134
- Burrows, A., Marley, M., Hubbard, W. B., et al. 1997, ApJ, 491, 856 (B97)
- Canuto, V.M. & Mazzitelli, I. 1991, ApJ, 370, 295
- Canuto, V.M. & Mazzitelli, I. 1992, ApJ, 389, 724
- Casey, B.W., Mathieu, R.D., Vaz, L.P.R., Andersen, J., & Suntzeff, N.B. 1998, AJ, 115, 1617
- Caughlan, G.R. & Fowler, W.A. 1988, ADNDT, 40, 283
- Chabrier, G. & Baraffe, I. 1997 AA, 327, 1039
- Chabrier, G., Baraffe, I., Allard, F., & Hauschildt, P. H. 2000, ApJ, 542, 464
- Charbonnel, C., Dappen, W., Schaerer, D., Bernasconi, P.A., Maeder, A., Meynet, G., & Mowlavi, N. 1999, A&AS, 135, 405 (C99)
- Chlebowski, T. & Garmany, C.D. 1991, ApJ 368, 241
- Code, A.D., Bless, R.C., Davis, J., & Brown, R.H. 1976, ApJ 203, 417
- Cohen, M. & Kuhl, L.V. 1979, ApJS, 41, 743
- Copeland, H., Jensen, J.O., & Jorgensen, H.E. 1970, AA, 5, 12
- Covino, E., Catalano, S., Frasca, A., et al. 2000, AA, 361, L49
- Cox, A.N. & Giuli, R. 1968, Principles of Stellar Structure (New York: Gordon & Breach)
- Cox, A.N. & Tabor, J.E. 1976, ApJS, 31, 271
- D’Antona, F., & Mazzitelli, I. 1985, ApJ, 296, 502
- D’Antona, F., & Mazzitelli, I. 1994, ApJS, 90, 467 (DM94)
- D’Antona, F., & Mazzitelli, I. 1997, in Cool stars in Clusters and Associations, ed. R. Pallavicini, & G. Micela, Mem. S. A. It., 68, 807 (DM97)
- D’Antona, F., Ventura, P., & Mazzitelli, I., 2000, ApJL, 543, 77
- Daepfen, W., Mihalas, D., Hummer, D.G. & Mihalas, B.W. 1988, ApJ, 332, 261

- Delfosse, X., Forveille, T., Ségransan, D., J. -L. Beuzit, Udry, S., Perrier, C. & Mayor, M. 2000 A&A, 364, 217
- Di Benedetto, G.P. & Rabbia, Y. 1987 AA 188, 114
- Drummond, J., Milster, S., Ryan, P. & Roberts, L. C., Jr. 2003, ApJ, 585, 1007
- Dutrey, A., Guilloteau, S., & Simon, M. 2003, AA, 402, 1003
- Dyck, H.M., Benson, J.A., van Belle, G.T., & Ridgway, S.T. 1996 AJ 111, 1705
- Eggleton, P.P., Faulkner, J. & Flannery, B.P. 1973, AA, 23, 325
- Ezer, D. & Cameron, A.G.W. 1967, Can J Phys 45, 3429
- Ezer, D. & Cameron, A.G.W. 1967, Can J Phys 45, 3461
- Fernandes, J., Lebreton, Y., Baglin, A. & Morel, P. 1998, A&A, 338, 455
- Forestini, M. 1994, AA 285, 473 (F94)
- Fowler, W.A., Caughlan, G.R., & Zimmerman, B.A. 1975, ARAA 13, 69
- Gliese, W. 1969, Catalogue of Nearby Stars
- Gray, D. 1992, The Observation and Analysis of Stellar Photospheres (Cambridge: Cambridge University Press)
- Gray, D. 1994, PASP, 106, 1248
- Girardi, L., Bressan, A., Bertelli, G. & Chiosi, C. 2000, A&AS, 141, 371
- Griffin, R.F. 1985, Obs, 105, 226
- Gruzinov, A.V. & Bahcall, J.N. 1998, ApJ, 504, 996
- Guenther, D. B. & Demarque, P. 2000, ApJ, 531, 503
- Guenther, D. B., Demarque, P., Kim, Y.-C., & Pinsonneault, M. H. 1992, ApJ, 387, 372
- Harris, M.J., Fowler, W.A., Caughlan, G.R., & Zimmerman, B.A., 1983, ARAA, 21, 165
- Hartigan, P., Edwards, S. & Ghandour, L. 1995, ApJ, 452, 736
- Hartigan, P., Strom, K., & Strom, S. 1994, ApJ, 427, 961
- Hartmann, L., Cassen, P., Kenyon, S.J., 1997, ApJ, 475, 770
- Hauschildt, P.H., Allard, F., Baron, E. 1999, ApJ, 512, 377
- Henry, T.J. & McCarthy, D.W. 1993, AJ, 106, 773
- Heney, L., Vardya, M.S. & Bodenheimer, P. 1965, ApJ, 142, 841
- Herbig, G. H., Vrba, F. J. & Rydgren, A. E.
- Hill, G. & Ebbighausen, E.G. 1984, AJ, 89, 1256
- Hillenbrand, L.A., Meyer, M.R., & Carpenter, J.M. 2004, in preparation
- Hummer, D.G. & Mihalas, D. 1988, ApJ, 331, 794
- Humphreys, R.M., & McElroy, D. B. 1984, 284, 565
- Iben, I. 1965, ApJ, 141, 993
- Iglesias, C.A. & Rogers, F.J. 1996, ApJ, 464, 943
- Jaschek, M., Jaschek, C., & Andrillat, Y. 1988, A&AS, 72, 505
- Johns-Krull, C.M., Valenti, J.A., & Koresko, C. 1999, ApJ, 516, 900
- Johns-Krull, C.M., & Valenti, J.A. 2001, in Stellar Clusters and Associations: Convection, Rotation, and Dynamos
- Kenyon, S.J., Dobrzycka, D., & Hartmann, L. 1994, AJ, 108, 1872

- Kim, Y.-C., Demarque, P., Yi, S., & Alexander, D. 2002, *ApJS*, 143, 499
- Kurucz, R.L. 1991, in *Stellar Atmospheres: Beyond Classical Models*, ed. L. Crivellari, I. Hubeny, and D.G. Hummer (Dordrecht: Kluwer), p. 441
- Lacy, C. H. 1997, *AJ*, 113, 1406
- Lacy, C. H. 1997, *AJ*, 113, 1091
- Lacy, C. H. 1997, *AJ*, 114, 2140
- Lacy, C. H. 1997, *AJ*, 114, 1206
- Larson, R. 1972, *MNRAS*, 156, 437
- Lastennet, E. & Valls-Gabaud, D. 2002, *AA*, 396, 551
- Latham, D. W., Nordstroem, B., Andersen, et al. 1996, *A&A*, 314, 864
- Leggett, S.K., Allard, F., Berriman, G., Dahn, C.C., & Hauschildt, P.H. 1996, *ApJS*, 104, 117
- Lejeune, T., Cuisinier, F. & Buser, R. 1998, *AA*, 130, 65
- Liu, Q & Yang, Y. 2002, *AA*, 361, 226
- Luhman, K.L., Liebert, J., & Rieke, G.H. 1997, *ApJL*, 489, 165
- Luhman, K.L., Stauffer, J.R., Muench, A.A., Rieke, G.H., Lada, E.A., Bouvier, J., & Lada, C.J. 2003, *ApJ*, 593, 1093
- Marrese, P. M., Munari, U., Siviero, A., Milone, E.F., Zwitter, T., Tomov, T., Boschi, F., & Boeche, C. 2003, *A&A*, in press
- Magni, G. & Mazzitelli, I. 1979, *AA*, 72, 134
- Martín, E.L., Rebolo, R., & Magazzù 1994, *ApJ*, 436, 262
- Massey, P., Parker, J.W., & Garmany, C.D. 1989, *AJ* 98, 1305
- McAlister, H.A., Hartkopf, W.I., Mason, B.D. et al. 1995, *AJ*, 110, 366
- Mendes, L.T.S., D’Antona, F. & Mazzitelli, I., 1999, *AA*, 341, 174
- Mercer-Smith, J.A., Cameron, A.G.W., & Epstein, R.I. 1984, *ApJ*, 279, 363
- Mihalas, D., Dappen, W., & Hummer, D.G. 1988, *ApJ*, 331, 815
- Milone, E. F., Stagg, C. R. & Kurucz, R. L. 1992, *ApJS*, 79, 123
- Montalban, J., D’Antona, F., Kupka, F., & Heiter, U., 2004, *AA*, submitted
- Munari, U., Tomov, T., Zwitter, T., Milone, E.F., Kallrath, J., Marrese, P.M., Boschi, F., Prsa, A., Tomasella, L., & Moro, D. 2001, *AA*, 378, 477
- North, P., Studer, M. & Künzli, M. 1997, *A&A*, 324, 137
- Palla, F., & Stahler, S. W. 1993, *ApJ*, 418, 414 (PS93)
- Palla, F., & Stahler, S. W. 1999, *ApJ*, 525, 772 (PS99)
- Plez, B. 1992, *A&AS*, 94, 527
- Pols, O.R., Tout, C.T., Eggleton, P.P., Han, Z. 1995, *MNRAS*, 274, 964
- Popper, D.M. 1980, *ARAA*, 18, 115
- Popper, D.M. 1987, *ApJ*, 313, L81
- Popper, D. M. 1994, *AJ*, 108, 1091
- Prato, L., Simon, M., Mazeh, T., Zucker, S., & McLean, I.S. 2002, *ApJ*, 579, 99
- Prato, L., Greene, T.P., & Simon, M. 2003, *ApJ*, 584, 853
- Ribas, I., Jordi, C. & Torra, J. 1999, *MNRAS*, 309, 199

- Ribas, I., Jordi, C., Torra, J., & Gimenez, A. 2000, MNRAS, 313, 99
- Rogers, F.J. & Iglesias, C.A. 1992, ApJS, 79, 507
- Rogers, F.J., Swenson, F.J., & Iglesias, C.A. 1996, ApJ, 456, 902
- Saumon, D., Chabrier, G., & van Horn, H.M. 1995, ApJS, 99, 713
- Schaefer, G. H., Simon, M., Nelan, E. & Holfeltz, S. T. 2003, AJ, 126, 1971
- Siess, L. & Livio, M. 1997, ApJ, 490, 785
- Siess, L., Forestini, M., & Bertout, C. 1997, AA, 326, 1001
- Siess, L., Dufour, E., & Forestini, M. 2000, AA, 358, 593 (S00)
- Sills, A., Pinsonneault, M. H. & Terndrup, D.M. 2000, ApJ, 534, 335
- Simon, M., Dutrey, A., & Guilloteau, S. 2000, ApJ, 545, 1034
- Stahler, S.W., 1983, ApJ, 274, 822
- Stauffer, J.R., Hartmann, L.W., & Barrado y Navascues, D. 1995, ApJ, 454, 910
- Steffen, A. T., Mathieu, R. D., Lattanzi, M. G., et al. 2001, AJ, 122, 997
- Strassmeier, K.G., Hall, D.S., Fekel, F.C. & Scheck, M. 1993, A&AS, 100, 173
- Strom, K.M., Allen, L.E., Hughes, J. 1994, BAAS
- Stuwe, J. A. & Schulz, R. 1994, Astron. Nachr.,
- Swenson, F.J., Faulkner, J., Rogers, F.J., & Iglesias 1994, ApJ, 425, 286 (S93)
- Tamazian, V.S., Docobo, J.A., White, R.J., & Woitas, J., 2002, ApJ, 578, 925
- Tinney, C.G., Mould, J.R., & Reid, I.N. 1993, AJ, 105, 1045
- Tomkin, J., McAlister, H.A., Hartkopf, W.I., Fekel, F.C. 1987, AJ, 93, 1236
- Torres, G. & Ribas, I. 2002, ApJ, 567, 1140
- Torres, G. Stefanik, R. P. & Latham, D. W. 1997a, ApJ, 485, 167
- Torres, G. Stefanik, R. P., Andersen, J., Nordström, B., Latham, D. W. & Clausen, J. V. 1997b, AJ, 114, 2764
- Torres, G., Henry, T.J., Franz, O., & Wasserman, L.H. 1999, AJ, 117, 562
- Torres, G., Boden, A.F., Latham, D.W., Pan, M., & Stefanik, R.P. 2002, AJ, 124, 1716
- Valenti, J. Basri, G. & Johns, C. M. 1993, AJ, 106, 2024
- VandenBerg, D.A. 1983, ApJS, 51, 29
- VandenBerg, D.A. 1992, ApJ, 391, 685
- VandenBerg, D.A. & Clem, J.L. 2003, AJ, 126, 778
- VandenBerg, D.A., Swenson, F.J., Rogers, F.J., Iglesias, C., & Alexander, D.R. 2000, ApJ, 532, 430
- White, R. J., Ghez, A. M., Reid, I. N., & Schultz, G. 1999, ApJ, 520, 811
- Wilkling, B.A., Greene, T.P., & Meyer, M.R. 1999 AJ 117, 469
- Yi, S., Kim, Y.-C. & Demarque, P. 2003, ApJS, 144, 259
- Yi, S., Demarque, P., Kim, Y. -C., Lee, Y.-W., Ree, C. H., Lejeune, T., & Barnes, S. 2001, ApJS, 136, 417
- Zwitter, T., Munari, U., Marrese, P.M., Prsa, A., Milone, E.F., Boschi, F., Tomov, T. & Siviero,

A. 2003, AA, 404, 333

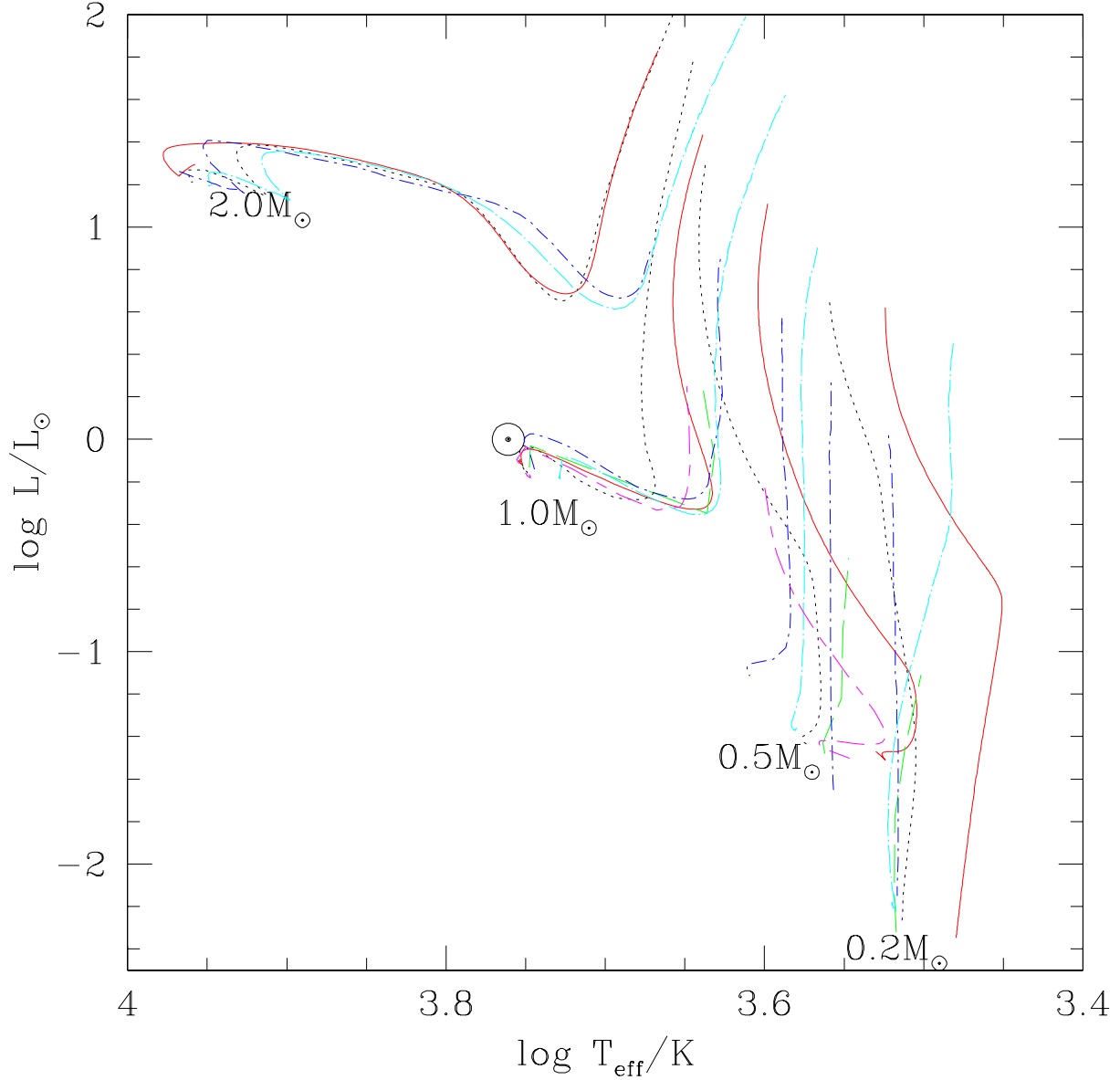


Fig. 1.— Variation between pre-main sequence contraction tracks for masses 0.2, 0.5, 1.0, and $2.0 M_{\odot}$. Line types indicate models of Swenson et al. (1993 – solid line), D’Antona & Mazzitelli (1997/1998 - dotted line), Baraffe et al. $\alpha=1.9$ (1998 – long-dash line), Palla & Stahler (1999 – dot-short-dash line), Siess et al. (2000 – dot-long-dash line), and Yi et al. (2003 – long-dash-short-dash line). Note that the Palla & Stahler models, for which no $0.5 M_{\odot}$ track is available, have both the 0.4 and the $0.6 M_{\odot}$ tracks plotted instead. Also note that the Yi et al. models do not extend as low as $0.2 M_{\odot}$.

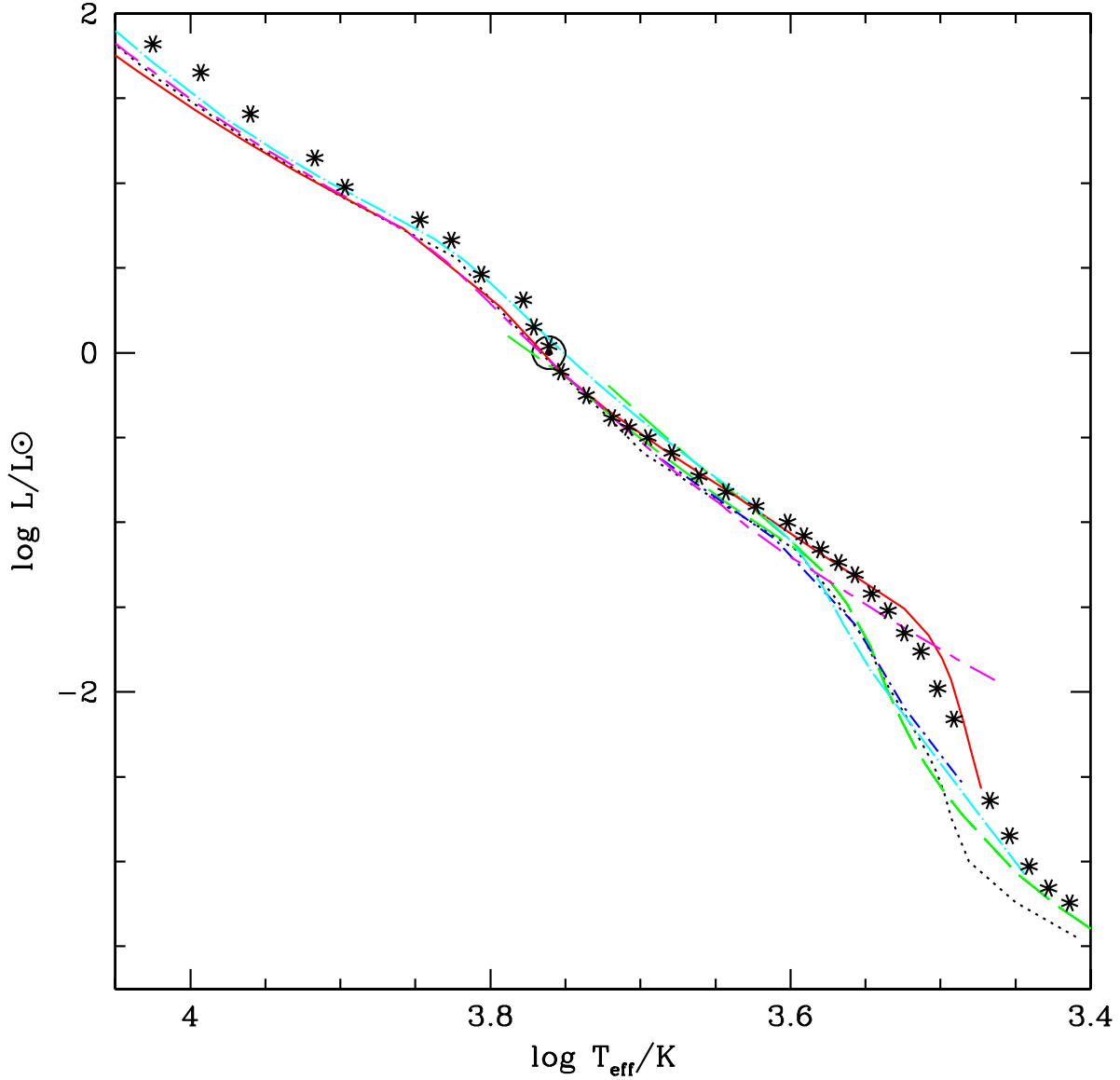


Fig. 2.— Comparison of the composite main sequences adopted by us using the various evolutionary models. Line types are the same as in Figure 1. Asterisks show the “empirical” main sequence derived from measurements of M_V and our adopted dwarf bolometric correction and temperature scales (see Appendix). Note that the empirical main sequence represents the average observed luminosity as a function of temperature along the main sequence and not necessarily the zero-age main sequence. Consequently, the highest mass main sequence stars are on average more evolved relative to zero-age than the average solar-mass main sequence star; this likely causes the apparent over-luminous location of the empirical main-sequence at higher masses. The Swenson et al. and the Yi et al. models extend cool enough to more accurately reproduce the low mass empirical main sequence compared to the other calculations; note however the “straight” nature of the Yi et al. main sequence which is at odds with the expected downturn due to H_2 dissociation.

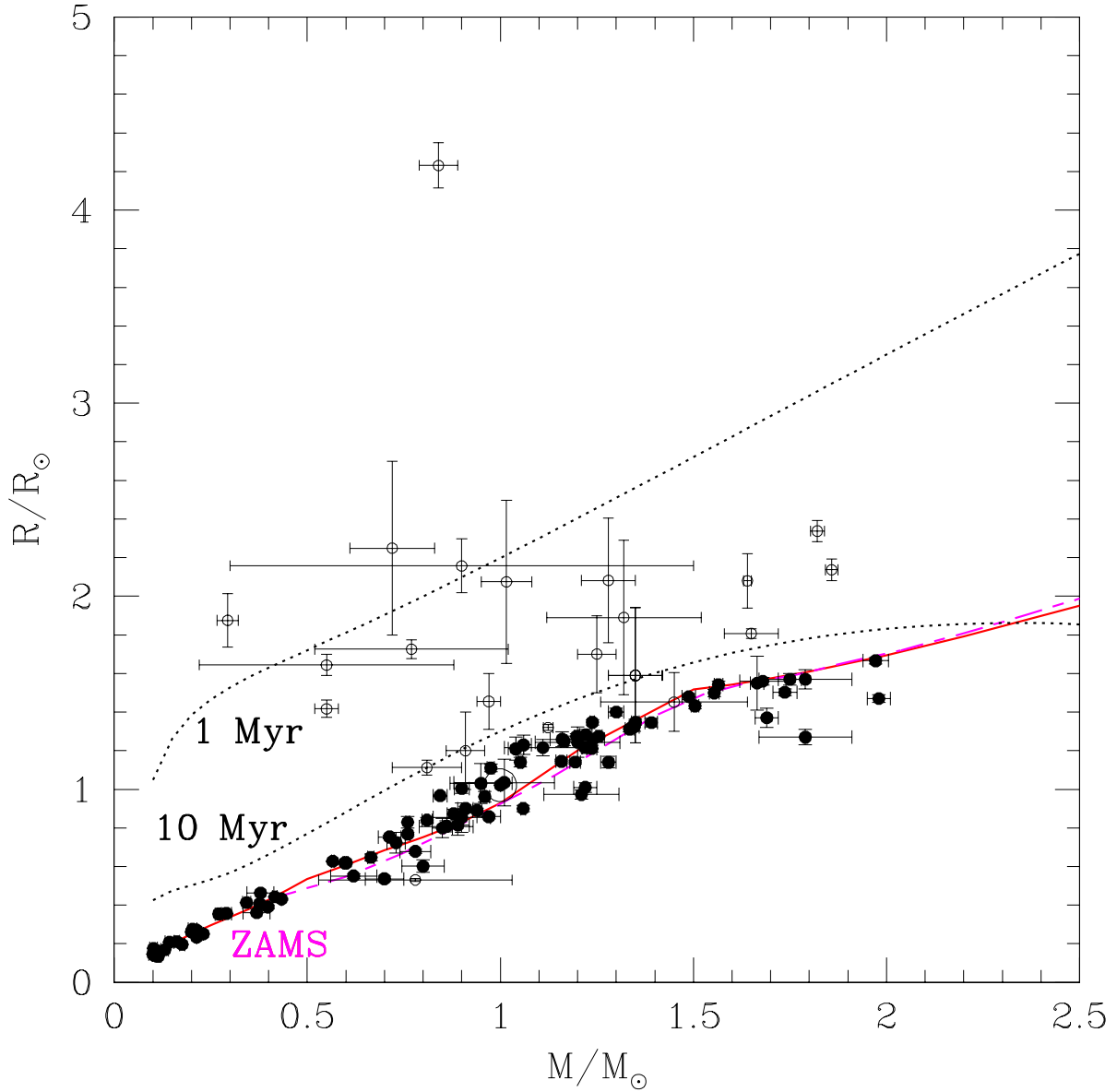


Fig. 3.— Mass and radius measurements for our sample stars. Open symbols represent pre-main sequence objects while filled symbols are main sequence stars. For the double-lined eclipsing systems both axes are fundamentally derived from observation whereas for the non-eclipsing systems the masses are fundamental but the radii are inferred from luminosity and effective temperature values in Table 1. The 1 and 10 Myr isochrones of D’Antona & Mazzitelli are indicated (dotted lines) to show the approximate change in radius with age as pre-main stars contract, as are the ZAMS from S93 (solid line) and Y² (dashed line) which most closely approximate the empirical main sequence in Figure 2.

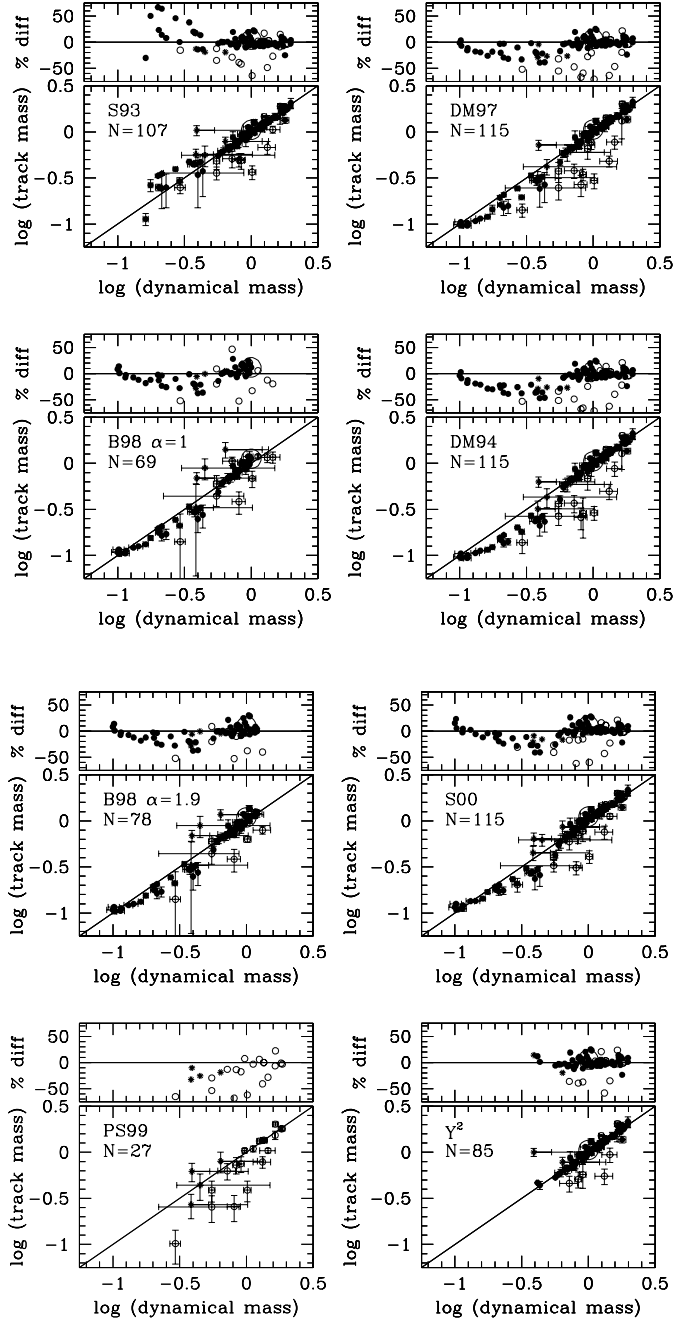


Fig. 4.— Comparison of dynamically determined masses with track-predicted masses in units of solar masses for main sequence (filled symbols) and pre-main sequence (open symbols) stars. Asterisks represent pre-main sequence binary systems whose individual components can be placed in the HR diagram but whose measured dynamical mass is that of the composite system; these systems have been plotted assuming an average dynamical mass of 1/2 the total dynamical mass and an average percentage mass difference of 1/2 the total. The Sun is also shown as the large open circle. Not all stars in Table 1 appear in all panels due to the variation between model calculations in the range of masses covered. The percentage mass difference in the upper panels is in the sense of track-predicted mass minus dynamical mass.

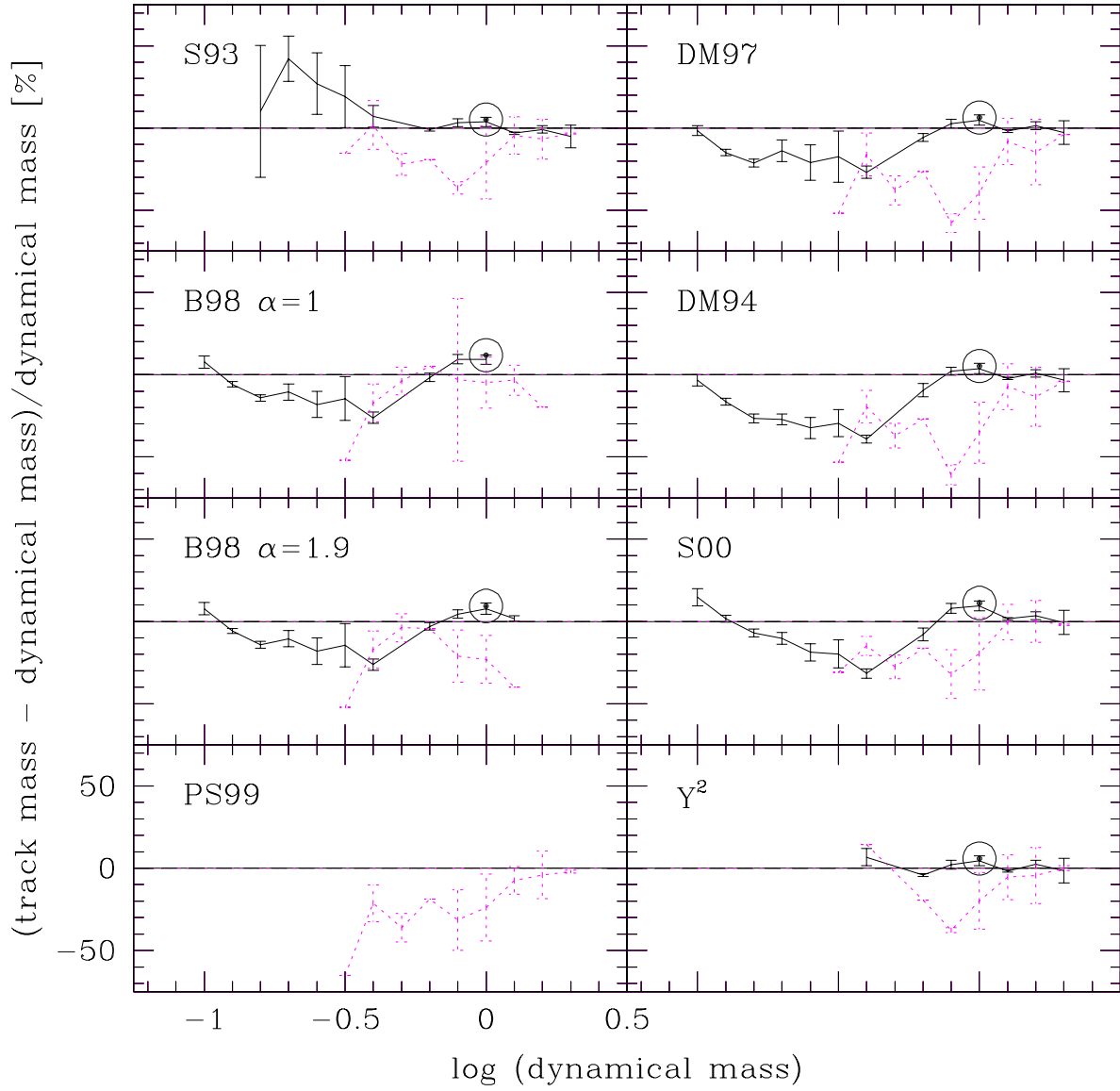


Fig. 5.— Mean percentage mass offset as a function of dynamically determined stellar mass for main sequence (solid lines) and pre-main sequence (dotted lines) stars; vertical error bars indicate the standard deviation of the mean. The difference values for the 4.5 Gyr old Sun are also shown as the large solar symbol.

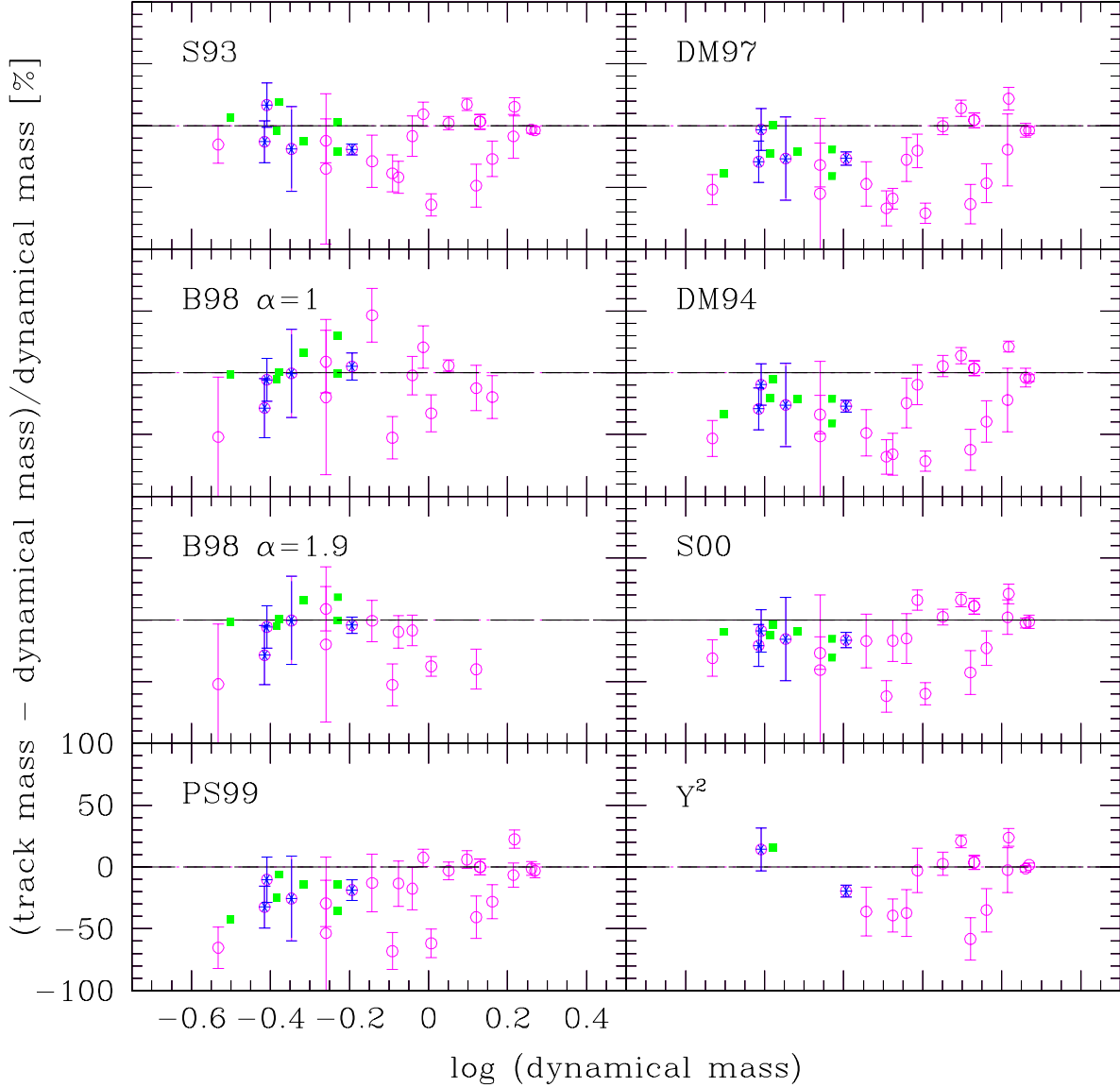


Fig. 6.— Percentage mass offset versus dynamically determined stellar mass for individual pre-main sequence stars. Vertical error bars indicate the root-sum-squared of the dynamical mass error and the track mass error, the latter estimated from the $\log L$ and $\log T$ errors. To illustrate the effects of temperature scale choice we show both the dwarf temperature scale adopted here (open circles) and the warmer Luhman (2003) temperature scale (filled squares) for stars later than M0, offset by +0.03 in \log dynamical mass for clarity. Note the change in scale compared to Figure 5.

Table 1. Sample and Stellar Parameters

Name	M/M _⊙	R/R _⊙	log g/cm s ⁻²	Type ^a	ref.	SpT	ref.	log T _{eff} ^b	log L/L _⊙	ref.	Ev. ^c	Comment
Candidate Main Sequence Stars												
WW Aur A	1.987 ± 0.034	1.883 ± 0.038	4.187 ± 0.019	EB	A91	A5m	A91	3.910± 0.015	1.140± 0.060	A91	3	
V909 Cyg A	1.980 ± 0.030	1.470 ± 0.020	4.403 ± 0.012	EB	L97c	A0	L97c	3.987± 0.021	1.230± 0.090	L97c	1	
KW Hya A	1.978 ± 0.036	2.125 ± 0.016	4.079 ± 0.013	EB	A91	A5m	A91	3.900± 0.006	1.220± 0.040	R03	3	
AI Hya B	1.978 ± 0.036	2.766 ± 0.017	3.850 ± 0.010	EB	A91	F0V	A91	3.869± 0.010	1.312± 0.036	R03	3	
V1647 Sgr B	1.972 ± 0.033	1.666 ± 0.017	4.289 ± 0.012	EB	A91	A1V	A91	3.949± 0.014	1.192± 0.057	R03	1	
TZ For B	1.949 ± 0.027	3.962 ± 0.088	3.532 ± 0.020	EB	A91	F7IV	A91	3.803± 0.007	1.360± 0.030	A91	3	
V624 Her B	1.881 ± 0.013	2.209 ± 0.034	4.024 ± 0.014	EB	A91	A7V	A91	3.900± 0.008	1.240± 0.040	A91	3	
MY Cyg B	1.811 ± 0.025	2.193 ± 0.050	4.014 ± 0.021	EB	A91	F0m	A91	3.846± 0.010	1.019± 0.045	R03	3	
GK Dra B	1.810 ± 0.109	2.830 ± 0.054	3.790 ± 0.041	EB	Z03	3.837± 0.004	1.188± 0.029	Z03	3	
51 Tau A	1.800 ± 0.130	O	T97a	3.859± 0.013	1.046± 0.040	T97a	3	Hyades member
WW Aur B	1.799 ± 0.025	1.883 ± 0.038	4.143 ± 0.018	EB	A91	A7m	A91	3.890± 0.015	1.060± 0.060	A91	3	
V477 Cyg A	1.790 ± 0.120	1.570 ± 0.050	4.300 ± 0.030	EB	GQ92	3.939± 0.015	1.100± 0.050	MQ92	1	
V477 Cyg B	1.790 ± 0.120	1.270 ± 0.040	4.360 ± 0.030	EB	GQ92	3.826± 0.015	0.470± 0.050	MQ92	1	
MY Cyg A	1.786 ± 0.030	2.193 ± 0.050	4.008 ± 0.021	EB	A91	F0m	A91	3.850± 0.010	1.035± 0.045	R03	3	
V909 Cyg B	1.750 ± 0.030	1.570 ± 0.030	4.288 ± 0.017	EB	L97c	A2	L97c	3.944± 0.016	1.120± 0.070	L97c	1	
IQ Per B	1.737 ± 0.031	1.503 ± 0.017	4.323 ± 0.013	EB	A91	A6V	A91	3.906± 0.008	0.850± 0.040	R03	1	
OO Peg A	1.720 ± 0.030	2.190 ± 0.080	3.990 ± 0.040	EB	M01	3.943± 0.007	1.388± 0.044	M01	3	
OO Peg B	1.690 ± 0.030	1.370 ± 0.050	4.390 ± 0.040	EB	M01	3.939± 0.009	0.964± 0.048	M01	1	
V526 Sgr B	1.680 ± 0.060	1.560 ± 0.020	4.280 ± 0.020	EB	L97b	3.940± 0.005	1.100± 0.030	L97b	1	
TV Nor B	1.665 ± 0.018	1.550 ± 0.014	4.278 ± 0.012	EB	N97	3.892± 0.006	0.902± 0.035	N97	1	
PV Pup A	1.565 ± 0.011	1.542 ± 0.018	4.257 ± 0.010	EB	A91	A8V	A91	3.840± 0.010	0.689± 0.041	R03	1	
V442 Cyg A	1.564 ± 0.024	2.072 ± 0.034	3.999 ± 0.016	EB	A91	F1V	A91	3.839± 0.006	0.940± 0.030	R03	3	
PV Pup B	1.554 ± 0.013	1.499 ± 0.018	4.278 ± 0.011	EB	A91	A8V	A91	3.841± 0.010	0.668± 0.041	R03	1	
RZ Cha A	1.518 ± 0.021	2.264 ± 0.017	3.909 ± 0.009	EB	A91	F5V	A91	3.816± 0.010	0.926± 0.041	R03	3	
RZ Cha B	1.509 ± 0.027	2.264 ± 0.017	3.907 ± 0.010	EB	A91	F5V	A91	3.816± 0.010	0.926± 0.041	R03	3	
TZ Men B	1.504 ± 0.010	1.432 ± 0.015	4.303 ± 0.009	EB	A91	A8V	A91	3.857± 0.012	0.692± 0.070	R03	1	
KW Hya B	1.488 ± 0.017	1.480 ± 0.014	4.270 ± 0.010	EB	A91	F0V	A91	3.836± 0.007	0.637± 0.029	R03	1	
BW Aqr A	1.488 ± 0.022	2.064 ± 0.044	3.981 ± 0.020	EB	A91	F7V	A91	3.800± 0.007	0.782± 0.034	R03	3	
GK Dra A	1.460 ± 0.066	2.431 ± 0.042	3.830 ± 0.033	EB	Z03	3.851± 0.004	1.112± 0.030	Z03	3	
DM Vir A	1.454 ± 0.008	1.763 ± 0.017	4.108 ± 0.009	EB	L96	F7V	A91	3.806± 0.010	0.700± 0.030	R03	3	
DM Vir B	1.448 ± 0.008	1.763 ± 0.017	4.106 ± 0.009	EB	L96	F7V	A91	3.806± 0.010	0.700± 0.030	R03	3	
CD Tau A	1.442 ± 0.016	1.798 ± 0.017	4.087 ± 0.010	EB	R99	F6V	R99	3.792± 0.004	0.630± 0.020	R99	3	
AD Boo A	1.438 ± 0.016	1.614 ± 0.012	4.180 ± 0.011	EB	L97	3.805± 0.006	0.590± 0.030	L97	3	
V442 Cyg B	1.410 ± 0.023	1.662 ± 0.033	4.146 ± 0.019	EB	A91	F2V	A91	3.833± 0.006	0.720± 0.030	R03	3	
V1143 Cyg A	1.391 ± 0.016	1.346 ± 0.023	4.323 ± 0.016	EB	A91	F5V	A91	3.820± 0.008	0.491± 0.035	R03	1	

Table 1—Continued

Name	M/M _⊙	R/R _⊙	log g/cm s ⁻²	Type ^a	ref.	SpT	ref.	log T _{eff} ^b	log L/L _⊙	ref.	Ev. ^c	Comment
BW Aqr B	1.386 ± 0.021	1.788 ± 0.043	4.075 ± 0.022	EB	A91	F8V	A91	3.807± 0.007	0.685± 0.035	R03	3	
CD Tau B	1.368 ± 0.016	1.584 ± 0.020	4.174 ± 0.012	EB	R99	F6V	R99	3.792± 0.004	0.520± 0.020	R99	3	
YZ Cas B	1.350 ± 0.010	1.348 ± 0.015	4.309 ± 0.010	EB	A91	F2V	A91	3.821± 0.016	0.496± 0.065	R03	1	
V1143 Cyg B	1.347 ± 0.013	1.323 ± 0.023	4.324 ± 0.016	EB	A91	F5V	A91	3.816± 0.008	0.460± 0.035	R03	1	
EE Peg B	1.335 ± 0.011	1.312 ± 0.013	4.328 ± 0.009	EB	A91	F5V	A91	3.802± 0.005	0.396± 0.022	R03	1	
IT Cas A	1.330 ± 0.009	1.593 ± 0.015	4.158 ± 0.009	EB	L97d	F5V	L97d	3.811± 0.007	0.601± 0.035	L97d	3	
IT Cas B	1.328 ± 0.008	1.560 ± 0.040	4.175 ± 0.020	EB	L97d	F5V	L97d	3.811± 0.007	0.583± 0.047	L97d	3	
V505 Per A	1.300 ± 0.020	1.400 ± 0.020	4.260 ± 0.010	EB	M01	3.808± 0.003	0.456± 0.016	M01	1	
V505 Per B	1.280 ± 0.020	1.140 ± 0.030	4.430 ± 0.010	EB	M01	3.807± 0.004	0.280± 0.020	M01	1	
V570 Per A	1.280 ± 0.030	1.640 ± 0.160	4.120 ± 0.050	EB	M01	3.810± 0.010	0.600± 0.072	M01	3	
HS Hya A	1.2552 ± 0.0078	1.2747 ± 0.0072	4.3259 ± 0.0056	EB	T97b	3.8129± 0.0033	0.415± 0.014	T97b	1	
RT And A	1.240 ± 0.030	1.260 ± 0.015	4.335 ± 0.015	EB	P94	F8V	S93	3.785± 0.015	0.290± 0.060	P94	1	CABS
UX Men A	1.238 ± 0.006	1.347 ± 0.013	4.272 ± 0.009	EB	A91	F8V	A91	3.785± 0.007	0.351± 0.029	R03	1	
AD Boo B	1.237 ± 0.013	1.211 ± 0.018	4.364 ± 0.019	EB	L97	3.775± 0.007	0.220± 0.040	L97	1	
AI Phe B	1.231 ± 0.005	2.931 ± 0.007	3.593 ± 0.003	EB	M92	F7V	A91	3.712± 0.013	0.730± 0.050	M92	3	
FL Lyr A	1.221 ± 0.016	1.282 ± 0.028	4.309 ± 0.020	EB	A91	F8V	A91	3.789± 0.007	0.320± 0.030	A91	1	
V570 Per B	1.220 ± 0.030	1.010 ± 0.025	4.550 ± 0.120	EB	M01	3.793± 0.013	0.080± 0.176	M01	1	
HS Hya B	1.2186 ± 0.0070	1.2161 ± 0.0071	4.3539 ± 0.0057	EB	T97b	3.8062± 0.0034	0.347± 0.015	T97b	1	
UV Leo A	1.210 ± 0.097	0.973 ± 0.024	4.540 ± 0.053	EB	Z03	...	Z03	3.787± 0.005	0.060± 0.038	Z03	1	
HR 6697 A	1.200 ± 0.110	O	P00	G0V	Mc95	3.771± 0.015	0.211± 0.040	Mc95	1	
UX Men B	1.198 ± 0.007	1.274 ± 0.013	4.306 ± 0.009	EB	A91	F8V	A91	3.781± 0.007	0.287± 0.029	R03	1	
EW Ori A	1.194 ± 0.014	1.141 ± 0.011	4.401 ± 0.010	EB	A91	G0V	A91	3.776± 0.007	0.170± 0.030	R03	1	
AI Phe A	1.190 ± 0.006	1.762 ± 0.007	4.021 ± 0.004	EB	M92	K0IV	A91	3.800± 0.010	0.640± 0.040	M92	3	
BH Vir A	1.165 ± 0.008	1.250 ± 0.025	4.340 ± 0.020	EB	P97	...	P97	3.789± 0.005	0.280± 0.030	R03	1	
α Cen A	1.160 ± 0.031	O	P00	G2V	P00	3.761± 0.004	0.181± 0.017	GD00	1	
EW Ori B	1.158 ± 0.014	1.145 ± 0.011	4.384 ± 0.010	EB	P97	G5V	A91	3.762± 0.007	0.080± 0.030	R03	1	
UV Leo B	1.110 ± 0.100	1.216 ± 0.043	4.310 ± 0.055	EB	Z03	...	Z03	3.759± 0.004	0.140± 0.045	Z03	1	
V432Aur B	1.060 ± 0.020	2.130± 0.140	3.810± 0.060	EB	M03	3.771 ± 0.007	0.708 ± 0.092	M03	3	
UWLMI A	1.060 ± 0.020	1.230± 0.050	4.280± 0.030	EB	M03	3.813 ± 0.007	0.368 ± 0.076	M03	1	
V818 Tau A	1.059 ± 0.006	0.900 ± 0.016	4.554 ± 0.016	EB	TR02	G6V	G85	3.743± 0.008	-0.169± 0.035	TR02	1	Hyades member; CABS
BH Vir B	1.052 ± 0.006	1.140 ± 0.025	4.350 ± 0.020	EB	P97	...	P97	3.750± 0.006	0.090± 0.060	R03	1	
UWLMI B	1.040 ± 0.020	1.210± 0.060	4.290 ± 0.040	EB	M03	3.813 ± 0.007	0.356 ± 0.080	M03	1	
CNLyn A	1.040 ± 0.020	1.800± 0.210	3.940 ± 0.100	EB	M03	3.813 ± 0.007	0.704 ± 0.120	M03	3	
CNLyn B	1.040 ± 0.020	1.800± 0.210	3.940 ± 0.100	EB	M03	3.813 ± 0.007	0.704 ± 0.112	M03	3	
χ Dra A	1.030 ± 0.050	O	P00	F7V	T87	3.742± 0.015	0.258± 0.047	T87	3	
Sun	1.000 ± 0.000	G2	...	3.761± 0.001	0.000± 0.007	G92	1	

Table 1—Continued

Name	M/M _⊙	R/R _⊙	log g/cm s ⁻²	Type ^a	ref.	SpT	ref.	log T _{eff} ^b	log L/L _⊙	ref.	Ev. ^c	Comment
V432Aur A	0.980 ± 0.020	1.390 ± 0.080	4.140 ± 0.06	EB	M03	3.785 ± 0.007	0.396 ± 0.088	M03	3	
UV Psc A	0.975 ± 0.009	1.110 ± 0.020	4.335 ± 0.016	EB	P97	G4-6V	S93	3.762 ± 0.007	0.090 ± 0.030	P97	1	CABS
α Cen B	0.970 ± 0.030	O	P00	K1V	P00	3.724 ± 0.004	-0.300 ± 0.011	GD00	1	
CG Cyg A	0.940 ± 0.012	0.890 ± 0.013	4.512 ± 0.014	EB	P94	G9.5V	S93	3.721 ± 0.015	-0.260 ± 0.060	P94	1	CABS
FL Lyr B	0.960 ± 0.012	0.962 ± 0.028	4.454 ± 0.026	EB	A91	G8V	A91	3.724 ± 0.008	-0.180 ± 0.040	A91	1	
η Cas A	0.950 ± 0.080	O	F98	G3V	F98	3.784 ± 0.004	0.099 ± 0.030	F98	1	
RT And B	0.910 ± 0.020	0.900 ± 0.013	4.484 ± 0.015	EB	P94	K0V	S93	3.675 ± 0.010	-0.435 ± 0.040	P94	1	CABS
HS Aur A	0.900 ± 0.019	1.004 ± 0.024	4.389 ± 0.023	EB	A91	G8V	A91	3.728 ± 0.006	-0.130 ± 0.030	A91	1	
70 Oph A	0.900 ± 0.074	O	P00	K0V	F98	3.726 ± 0.002	-0.296 ± 0.080	F98	1	
81 Cnc A	0.890 ± 0.029	O	P00	G8V	M96	3.736 ± 0.015	-0.296 ± 0.060	M96	1	
HS Aur B	0.879 ± 0.017	0.873 ± 0.024	4.500 ± 0.025	EB	A91	K0V	A91	3.716 ± 0.006	-0.300 ± 0.030	A91	1	
ξ Boo A	0.860 ± 0.070	O	F98	G8V	F98	3.744 ± 0.002	-0.272 ± 0.030	F98	1	
81 Cnc B	0.850 ± 0.026	O	P00	G8V	M96	3.736 ± 0.015	-0.313 ± 0.060	m96	1	
HD195987 A	0.844 ± 0.018	O	To02	...	To02	3.716 ± 0.008	-0.228 ± 0.001	To02	1	[Fe/H] = -0.5
CG Cyg B	0.810 ± 0.013	0.840 ± 0.014	4.505 ± 0.016	EB	P94	K3V	S93	3.674 ± 0.006	-0.510 ± 0.030	P94	1	CABS
HR 6697 B	0.800 ± 0.055	O	P00	K3V	Mc95	3.679 ± 0.015	-0.788 ± 0.128	Mc95	1	
70 Oph B	0.780 ± 0.040	O	P00	K5V	F98	3.638 ± 0.015	-0.848 ± 0.040	F98	1	
V818 Tau B	0.760 ± 0.006	0.768 ± 0.010	4.548 ± 0.011	EB	TR02	K6V	G85	3.645 ± 0.015	-0.775 ± 0.062	TR02	1	Hyades member; CABS
UV Psc B	0.760 ± 0.005	0.830 ± 0.030	4.480 ± 0.031	EB	P97	K0-K2V	S93	3.677 ± 0.007	-0.500 ± 0.040	P97	1	CABS
χ Dra B	0.730 ± 0.024	O	P00	K0V	T87	3.719 ± 0.030	-0.468 ± 0.105	T87	1	
Gl702 B	0.713 ± 0.029	O	H93	3.626 ± 0.0119	-0.805 ± 0.05	D00	1	
ξ Boo B	0.700 ± 0.050	O	F98	K4V	F98	3.638 ± 0.015	-1.052 ± 0.080	F98	1	
HD195987 B	0.665 ± 0.008	O	To02	...	To02	3.623 ± 0.021	-0.949 ± 0.076	To02	1	[Fe/H] = -0.5
η Cas B	0.620 ± 0.060	O	F98	K7V	F98	3.606 ± 0.016	-1.157 ± 0.080	F98	1	
YY Gem B	0.601 ± 0.005	0.619 ± 0.006	4.632 ± 0.008	EB	TR02	dM1e	S93	3.582 ± 0.011	-1.135 ± 0.009	TR02	1	CABS
YY Gem A	0.598 ± 0.005	0.619 ± 0.006	4.632 ± 0.008	EB	TR02	dM1e	S93	3.582 ± 0.011	-1.135 ± 0.009	TR02	1	CABS
Gl570 B	0.566 ± 0.003	O	F99	3.548 ± 0.0056	-1.276 ± 0.05	D00	1	
CU Cnc Aa	0.433 ± 0.002	0.432 ± 0.005	4.804 ± 0.011	EB	R03	M3.5V	R03	3.500 ± 0.021	-1.778 ± 0.083	R03	1	
Gl644 A	0.4155 ± 0.0057	O	Se00	3.524 ± 0.0036	-1.674 ± 0.05	D00	1	
CU Cnc Ab	0.398 ± 0.001	0.391 ± 0.009	4.854 ± 0.021	EB	R03	M3.5V	R03	3.495 ± 0.021	-1.884 ± 0.086	R03	1	
Gl661 A	0.379 ± 0.035	A	M98	3.509 ± 0.0028	-1.695 ± 0.05	D00	1	
Gl570 C	0.377 ± 0.002	O	F99	3.519 ± 0.0083	-1.768 ± 0.05	D00	1	
Gl661 B	0.369 ± 0.035	A	M98	3.526 ± 0.0039	-1.843 ± 0.05	D00	1	
Gl623 A	0.343 ± 0.011	O	D00	3.531 ± 0.0032	-1.707 ± 0.05	D00	1	
Gl831 A	0.291 ± 0.013	O	Se00	3.486 ± 0.0022	-2.014 ± 0.05	D00	1	
Gl860 A	0.271 ± 0.010	O	H99	3.507 ± 0.0023	-1.936 ± 0.05	D00	1	

Table 1—Continued

Name	M/M _⊙	R/R _⊙	log g/cm s ⁻²	Type ^a	ref.	SpT	ref.	log T _{eff} ^b	log L/L _⊙	ref.	Ev. ^c	Comment
CM Dra A	0.231 ± 0.001	0.252 ± 0.002	4.998 ± 0.002	EB	M96	M4Ve	S93	3.488±0.008	-2.301± 0.044	V97	1	
CM Dra B	0.214 ± 0.001	0.235 ± 0.002	5.025 ± 0.007	EB	M96	M4Ve	S93	3.488± 0.008	-2.360± 0.044	V97	1	
Gl747 A	0.214 ± 0.001	O	Se00	3.508±0.0026	-2.165± 0.05	D00	1	
Gl234 A	0.2027 ± 0.0106	O	D00	3.486±0.0018	-2.237± 0.05	D00	1	
Gl747 B	0.200 ± 0.001	O	Se00	3.504±0.0026	-2.213± 0.05	D00	1	
Gl860 B	0.176 ± 0.007	O	H99	3.495±0.0040	-2.497± 0.05	D00	1	
Gl831 B	0.162 ± 0.007	O	Se00	3.463±0.0022	-2.562± 0.05	D00	1	
Gl473 A	0.143 ± 0.011	A	T99	3.455±0.0021	-2.607± 0.05	D00	1	
Gl473 B	0.131 ± 0.010	A	T99	3.466±0.0026	-2.745± 0.05	D00	1	
Gl866 B	0.1145 ± 0.0012	O	Se00	3.453±0.0021	-2.837± 0.05	D00	1	
Gl623 B	0.114 ± 0.008	A	D00	3.453±0.0042	-2.986± 0.05	D00	1	
Gl234 B	0.1034 ± 0.0035	O	Se00	3.448±0.0019	-2.977± 0.05	D00	1	
Gl65 A	0.102 ± 0.010	A	H99	3.454±0.0020	-2.754± 0.05	D00	1	
Gl65 B	0.100 ± 0.010	A	H99	3.453±0.0022	-2.920± 0.05	D00	1	
Pre-Main Sequence Stars												
RS Cha A	1.858 ± 0.016	2.137 ± 0.055	4.047 ± 0.023	EB	A91	A8	M00	3.883± 0.010	1.144± 0.044	M00	2	
RS Cha B	1.821 ± 0.018	2.338 ± 0.055	3.961 ± 0.021	EB	A91	A8	M00	3.859± 0.010	1.126± 0.043	M00	2	
MWC 480	1.650 ± 0.070	D	Si00	A2-3	JJA88	3.948±0.015	1.243± 0.10	...	2	
TY CrA B	1.640 ± 0.010	2.080 ± 0.140	4.020 ± 0.050	EB	C98	...	C98	3.690± 0.035	0.380± 0.145	C98	2	
045251+3016 A	1.450 ± 0.190	O	St01	K5	St01	3.643±0.015	-0.167± 0.053	St01	2	
AK Sco A	1.350 ± 0.070	1.590 ± 0.350	...	SB	A03	F5	A89	3.813± 0.007	0.607± 0.050	A03	2	
AK Sco B	1.350 ± 0.070	1.590 ± 0.350	...	SB	A03	F5	A89	3.813± 0.007	0.607± 0.050	A03	2	
BP Tau	1.320 ± 0.200	D	Du03	K7	B90/H95	3.608±0.012	-0.780± 0.10	JVK99	2	
0529.4+0041 A	1.250 ± 0.050	1.700 ± 0.200	4.070 ± 0.100	EB	C00	K1-K2	C00	3.701± 0.009	0.243± 0.037	C00	2	
EK Cep B	1.124 ± 0.012	1.320 ± 0.015	4.250 ± 0.015	EB	P87	3.755± 0.015	0.190± 0.070	P87	2	
UZ Tau Aa	1.016 ± 0.065	DSB	Si00	M1	P02	3.557±0.015	-0.201± 0.124	P02	2	
0529.4+0041 B	0.910 ± 0.050	1.200 ± 0.200	4.240 ± 0.150	EB	C00	K7-M0	C00	3.604± 0.022	-0.469± 0.192	C00	2	
LkCa 15	0.970 ± 0.030	D	Si00	K5	H86	3.643±0.015	-0.165± 0.10	...	2	
GM Aur	0.840 ± 0.050	D	Si00	K7	B90/H95	3.602±0.015	0.598± 0.10	...	2	
045251+3016 B	0.810 ± 0.090	O	St01	3.535±0.015	-0.830± 0.086	St01	2	
DL Tau	0.720 ± 0.110	D	Si00	K7-M0	B90/H95	3.591±0.015	0.005± 0.10	...	2	
DM Tau	0.550 ± 0.030	D	Si00	M1	V93	3.557±0.015	-0.532± 0.10	...	2	
CY Tau	0.550 ± 0.330	D	Si00	M2	SS94	3.535±0.015	-0.491± 0.10	...	2	
UZ Tau Ab	0.294 ± 0.027	DSB	Si00	M4	P02	3.491±0.015	-0.553± 0.124	p02	2	
Pre-Main Sequence Composite Systems												
GG Tau Aa	(1.28 ± 0.07)×C	D	Si01	M0	HK03	3.580±0.015	-0.106± 0.10	...	2	

Table 1—Continued

Name	M/M _⊙	R/R _⊙	log g/cm s ⁻²	Type ^a	ref.	SpT	ref.	log T _{eff} ^b	log L/L _⊙	ref.	Ev. ^c	Comment
GG Tau Ab	(1.28 ± 0.07) × (1 - C)	D	Si01	M2	HK03	<i>3.535 ± 0.015</i>	-0.338 ± 0.10	...	2	
DF Tau A	(0.90 ± 0.60) × C	A	S03	M2	HK03	<i>3.535 ± 0.015</i>	-0.255 ± 0.10	...	2	
DF Tau B	(0.90 ± 0.60) × (1 - C)	A	S03	M2.5	HK03	<i>3.524 ± 0.015</i>	-0.162 ± 0.10	...	2	
FS Tau A	(0.78 ± 0.25) × C	A	Ta02	M0	HK03	<i>3.580 ± 0.015</i>	-1.293 ± 0.10	...	2	
FS Tau B	(0.78 ± 0.25) × (1 - C)	A	Ta02	M3.5	HK03	<i>3.502 ± 0.015</i>	-1.552 ± 0.10	...	2	
FO Tau A	(0.77 ± 0.25) × C	A	Ta02	M3.5	HK03	<i>3.502 ± 0.015</i>	-0.581 ± 0.10	...	2	
FO Tau B	(0.77 ± 0.25) × (1 - C)	A	Ta02	M3.5	HK03	<i>3.502 ± 0.015</i>	-0.609 ± 0.10	...	2	

^a Method used to determine the dynamical mass: EB = eclipsing binary system, O = astrometric + radial velocity orbit, A = astrometric orbit + distance estimate, D = disk kinematics, DSB = disk kinematics + doubled-lined spectroscopic binary

^b Main-sequence temperatures in italics are determined from colors; pre-main sequence temperatures in italics are determined from a spectral type.

^c Evolutionary status code: 1 = main sequence; 2 = pre-main sequence; 3 = post-main sequence / evolved.

References. — References: A91 = Anderson (1991); A03 = Alencar et al. (2003); A89 = Andersen et al. (1989); B90 = Basri & Batalha (1990); C98 = Casey et al. (1998); C00 = Covino et al. (2000); D00 = Delfosse, X. et al. (2000); Dr03 = Drummond et al. (2003); Du03 = Dutrey et al. (2003); F98 = Fernandes et al. (1998); F99 = Forveille et al. (1999); G85 = Griffin (1985); G169 = Gliese (1969); GD00 = Guenther & Demarque (2000); H95 = Hartigan et al. (1995); H86 = Herbig et al. (1986); H93 = Henry et al. (1993); H99 = Henry et al. (1999); HE84 = Hill & Ebbighausen (1984); HK03 = Hartigan & Kenyon (2003); JJA88 = Jaschek et al. (1988); L96 = Latham (1996); L97a = Lacy (1997a); L97b = Lacy (1997b); L97c = Lacy (1997c); L97d = Lacy (1997d); Mc95 = McAlister et al. (1995); M98 = Martin et al. (1998); M01 = Munari (2001); M03 = Marrese et al. (2003); M92 = Milone et al. (1992); P87 = Popper (1987); P02 = Prato et al. (2002); P94 = Popper (1994); R99 = Ribas et al. (1999); Se00 = S´ egransan et al. (2000); Si00 = Simon et al. (2001); St01 = Steffen et al. (2001); SS94 = Stuwe & Schulz (1994); S03 = Schaefer et al. (2003); S93 = Strassmeier et al. (1993); Ta02 = Tamazian et al. (2002); T87 = Tomkin et al. (1987); T97a = Torres et al. (1997a); T97b = Torres et al. (1997b); T99 = Torres et al. (1999); TR02 = Torres & Ribas (2002); To02 = Torres et al. (2002); V93 = Valenti et al. (1993); Z03 = Zwitter et al. (2003)